The University of Chicago

DEPARTMENT OF THE GEOPHYSICAL SCIENCES

*

THE FREE OSCILLATIONS OF LAKE ERIE

by

George W. Platzman

and

Desiraju B. Rao

*

Technical Report Number 8

to

United States Weather Bureau

(Grant WBG-7)

September 1963

The University of Chicago

*

TECHNICAL REPORTS AND PUBLICATIONS OF THE DYNAMICAL PREDICTION GROUP

Department of the Geophysical Sciences

*Out of print. + Thesis.

1. Akira Kasahara: The numerical prediction of hurricane movement with the barotropic model. (Technical Report to U. S. Weather Bureau, November 1956). Journal of Meteorology, 14 (1957) 386-402.

*2. Akira Kasahara: A method for solving the balance equation with the relative vorticity as a carrying parameter. (Technical Report to U. S. Weather Bureau, March 1957). Included in number 10 (see below).

*3. Gene E. Birchfield: Numerical prediction of hurricane movement with the use of a fine grid. (Technical Report to U. S. Weather Bureau, March 1957). Included in number 15b (see below).

*4. Akira Kasahara: A test of the barotropic numerical prediction of hurricane movement at the 700-mb level. (Technical Report to U. S. Weather Bureau, June 1957). Included in number 10 (see below).

5. Y. Ogura: On the truncation error which arises from the use of finite differences in the Laplacian operator. (Technical Report to U. S. Weather Bureau, July 1957). Journal of Meteorology, 15 (1958) 475-480.

*6. Ferdinand Baer and George W. Platzman: The extended numerical integration of a simple barotropic model. Part I. Program. (Technical Report to National Science Foundation, April 1958). Included in number 14b (see below).

7. George W. Platzman: An approximation to the product of discrete functions. (Technical Report to National Science Foundation, April 1958). Journal of Meteorology, 18 (1961) 31-37.

8. George W. Platzman: A numerical computation of the surge of 26 June 1954 on Lake Michigan. (Technical Report to U. S. Weather Bureau, June 1958). Geophysica, 6 (1958) 407-438.

9. George W. Platzman: The lattice structure of the finite-difference primitive and vorticity equations. (Technical Report to U. S. Weather Bureau, August 1958). Monthly Weather Review, 86 (1958) 285-292.

10. Akira Kasahara: A comparison between geostrophic and nongeostrophic numerical forecasts of hurricane movement with the barotropic steering model. (Technical Report to U. S. Weather Bureau, August 1958). Journal of Meteorology, 16 (1959) 371-384.

11. George W. Platzman: A solution of the nonlinear vorticity equation. (Technical Report to National Science Foundation, August 1958). The Rossby Memorial Volume, 326-332. Rockefeller Institute Press, 1959.

*12. John M. Mihaljan: A study of the finite difference solution of the forced wave equation. (Technical Report to U. S. Weather Bureau, September 1958).

+13. Chester P. Jelesnianski: The July 6, 1954 water wave on Lake Michigan generated by a pressure jump passage. M.S. Thesis, December 1958.

*14a. Ferdinand Baer: The extended numerical integration of a simple barotropic model. Part II. Results. (Technical Report to National Science Foundation, December 1958). Included in number 14b (see below).

14b. Ferdinand Baer: The extended numerical integration of a simple barotropic model. Journal of Meteorology, 18 (1961) 319-339.

*15a. Gene E. Birchfield: Further studies of barotropic numerical prediction of hurricane movement with the use of a fine grid. (Technical Report to U. S. Weather Bureau, December 1958). Included in number 15b (see below).

15b. Gene E. Birchfield: Numerical prediction of hurricane movement with the use of a fine grid. Journal of Meteorology, 17 (1960) 406-414.

(continued on inside back cover)

CONTENTS

*

Page

THE FREE OSCILLATIONS OF LAKE ERIE

by

George W. Platzman and Desiraju B. Rao

The University of Chicago

*

ABSTRACT

The longitudinal free oscillations of Lake Erie are investigated theoretically by numerical integration of the channel equations, and observationally by analysis of water-level covariance spectra. Good agreement is obtained between computed and observed periods of the first four modes, as well as between computed and observed amplitude.

Particular attention is given to influence of the earth's rotation and to the effect of friction. The general conclusions are that the earth's rotation transforms the lowest longitudinal mode into an amphidromic wave with counterclockwise rotation of cotidal lines, but does not significantly affect the period of any mode. Friction increases the period by at most a few per cent. Cross-spectral analyses of water-level data give high-water phases of the lowest mode that are qualitatively (and in some cases quantitatively) in good accord with phases computed on the assumption that the transverse profile slope is quasi-geostrophic, and thus support the conclusion that this mode is a "positive" amphidromic wave.

1. Introduction

One of the most conspicuous longitudinal free oscillations of the Great Lakes is that of Lake Erie, the location of which is shown in figure 1. (The configuration of the Lake can be seen in more detail in figure 4.) The Lake lends itself to a division into three sub-basins: a small, shallow Western Basin with many reefs and islands; a flat, unrestricted Central Basin; and a small Eastern Basin which is the deepest of the three. Quantitative aspects of this structure are given in table 1. The mean depth of the Lake as a whole is only about 61 feet (much less than that of any of the other Great Lakes); as a result, wind action is very pronounced.

A good indication of the prominence of longitudinal oscillations is provided by water-level records at Buffalo and Toledo, situated at opposite ends of the longitudinal axis. The lowest (uninodal) mode, with a period of about 14 hours, is a well-known feature of such records, as has been noted by many investigators. In figure 2, which shows one month of record (September 1958), a series of 14-hour oscillations is initiated on the 10th and again on the 28th day of the month. A period of about 9 hours also has been detected by careful visual inspection of the records. The

TABLE 1. Physical characteristics of Lake Erie Basin.*

	WESTERN BASIN	CENTRAL BASIN	EASTERN BASIN	ENTIRE BASIN
Volume				
10^{12} cubic feet:	0.8	10.6	5.4	16.8
per cent:	5	63	32	100
Area				
10^{10} square feet:	3.5	17.4	6.7	27.6
per cent	13	63	24	100
Depth in feet				
mean:	24.2	60.7	79.9	60.7
maximum:	48	84	210	210
Dimensions in statute miles				
length (maximum):	50	132	85	241
width (maximum:	40	57	42	57
width (mean):	25	47	28	41

*From data given by Verber (1960). Mean depths are based upon a lake level of 568.6 feet MSL-IGLD (International Great Lakes Datum of 1955).

theoretical analysis given below confirms that the 9-hour oscillation is the binodal mode.

At the end of this paper a brief historical summary is given, in which are listed the principal assessments of observed and computed periods of the free oscillations of Lake Erie that are to be found in the literature on this subject. It is a curious fact --- but true, so far as the writers have been able to determine --- that all past theoretical estimates have been based upon nothing more than the Merian or DuBoys formulas, which are well known to be inapplicable to the lowest modes of many lakes. The more exact methods of computation initiated by Chrystal and perfected by Defant, Hidaka and others have been applied in the past half century virtually to every important lake in the world, but the writers know of only one application of these methods to the Great Lakes of the United States, namely that of F. Defant (1954) on Lake Michigan.

In the present paper the free oscillations of Lake Erie are investigated by means of classical methods of numerical integration of the dynamical equations for flow in a channel of gradually varying section. A very brief outline of the procedure used here is given, but it has not been thought necessary to cite

references because the methods are well known in theoretical limnology as well as in various branches of applied mathematics. In his recent book, A. Defant (1961) has given an excellent account of the entire subject.

In the next two sections the method of computation is outlined and the basic numerical results are presented. Then corrections resulting from the earth's rotation and from friction are considered, as well as perturbations from variation of mean lake level and from end conditions. Finally, a verification analysis is given, in which the results of numerical computation are compared with observed wave characteristics derived from analysis of water-level covariance spectra.

2. Integration procedure

The linearized momentum and mass equations for flow in a channel of gradually varying section are

$$\frac{\partial \hat{Q}}{\partial t} = - gS \frac{\partial \hat{\zeta}}{\partial x} \qquad (2.1)$$

$$\frac{\partial \hat{\zeta}}{\partial t} = - \frac{1}{b} \frac{\partial \hat{Q}}{\partial x} , \qquad (2.2)$$

where $\hat{Q}(x,t)$ is the volume transport through a vertical section of the channel, $S(x)$ is the section area, $\hat{\zeta}(x,t)$ is the mean water level across the section (relative to undisturbed level), and $b(x)$ is the surface breadth of the section (figure 3). The x -axis is locally tangent to the principal axis of the channel, which may be regarded as coinciding with the troughline of the channel or with the direction of flow near the channel center. The vertical section is locally perpendicular to the flow at each point of its surface.

The free oscillations are assumed expressible in the form appropriate for a closed basin:

$$\hat{Q}(x,t) = Q(x) \sin \sigma t \qquad (2.3)$$

$$\hat{\zeta}(x,t) = \zeta(x) \cos \sigma t \,, \qquad (2.4)$$

where Q, ζ are the x-dependent parts of $\hat{Q}, \hat{\zeta}$ and σ is the oscillation frequency. The dynamical equations (2.1, 2) then reduce to

$$-\frac{\sigma}{gS} Q = \frac{d\zeta}{dx} \qquad (2,5)$$

$$\sigma b \zeta = \frac{dQ}{dx} \,. \qquad (2,6)$$

With boundary conditions $Q=0$ at $X=0$ and $X=L$, equations (2.5, 6) pose a characteristic-value problem for determination of σ.

The dotted line in figure 4 shows the principal axis of Lake Erie. In the calculations to be described presently, values of profile ζ are obtained on each of 40 sections identified in figure 4 by the solid lines, and values of transport Q are obtained at each of 39 sections identified by broken lines. The ζ-sections are drawn to intersect the principal axis at points spaced uniformly with an interval $1/3 \times 10^5$ feet (6.31 statute miles). Q-sections are drawn midway between ζ-sections. The section area S was determined at each Q-section and the surface width b at each ζ-section, with U. S. Lake Survey chart L.S.3 as the basis for measurement (scale 1:400,000). The results are shown in figure 5.

In the standard procedure for numerical integration of (2.5, 6) one replaces the derivatives on the right by central differences:

$$-\frac{\sigma}{gS_i}Q_i = \frac{\zeta_{i+1}-\zeta_{i-1}}{\Delta x}\ ;\quad i=2(2)78 \qquad (2.7)$$

$$\sigma B_i \zeta_i = \frac{Q_{i+1}-Q_{i-1}}{\Delta x}\ ;\quad i=1(2)79 \qquad (2.8)$$

or, after re-arrangement:

$$\zeta_{i+1} = \zeta_{i-1} - \sigma c_i Q_i\ ;\quad i=2(2)78 \qquad (2.9)$$

$$Q_{i+1} = Q_{i-1} - \sigma d_i \zeta_i\ ;\quad i=1(2)79\ , \qquad (2.10)$$

where $c \equiv \Delta x/gS$ and $d \equiv -B\Delta x$. To solve (2.9, 10) by successive approximation one assigns to ζ_1 a convenient value (which is arbitrary because the equations are homogeneous); then a trial value is given to the frequency σ (or period $T \equiv 2\pi/\sigma$) and Q_2 is computed from (2.10) with $Q_0 = 0$ as boundary condition. Then ζ_3 is computed from (2.9), and by alternate use of (2.9) and (2.10) we arrive at Q_{80} , which should be zero as a boundary condition. If $Q_{80} \neq 0$, we alter the value of σ and compute Q_{80} again. This procedure is repeated until, by interpolation or otherwise, a sufficiently accurate value of σ is obtained. With the use of a high-speed computer this method

is simple and efficient.

A departure from the standard procedure just described was made in order to deal with the effect of Long Point Bay, the mouth of which coincides with ζ-section $i = 21$ (figure 4). The mouth of the Bay contributes 0.62×10^7 ft^2 to the area of section 21 and the main channel contributes 1.33×10^7 ft^2, so the main channel covers only about 68 per cent of the area of the section. To take account of this configuration, we visualize the Lake as divided into three regions: the Eastern Basin, for which $0 \leq i \leq 21$; Long Point Bay, for which $21 \leq i' \leq 26$; and the Central and Western Basins for which $21 \leq i \leq 80$. The channel equations then are formulated for each region separately, with joining conditions expressing continuity of profile and transport at $i = 21$, the section common to the three regions.

Using primes to identify quantities pertaining to Long Point Bay, it is clear that in place of (2.7, 8) we have now:

<u>Eastern, Central and Western Basins</u>

$$-\frac{\sigma}{gS_i} Q_i = \frac{\zeta_{i+1} - \zeta_{i-1}}{\Delta x} \; ; \begin{pmatrix} i = 2(2)20 \\ i = 20(2)78 \end{pmatrix} \qquad (2.11)$$

$$\sigma B_i \zeta_i = \frac{Q_{i+1} - Q_{i-1}}{\Delta x} \; ; \begin{pmatrix} i = 1(2)19 \\ i = 23(2)79 \end{pmatrix} \qquad (2.12)$$

Section 21

$$\sigma b_{21} \zeta_{21} = \frac{Q'_{22} + Q_{22} - Q_{20}}{\Delta x} \qquad (2.13)$$

Long Point Bay

$$-\frac{\sigma}{g S'_i} Q'_i = \frac{\zeta'_{i+1} - \zeta'_{i-1}}{\Delta x}; \quad i = 22(2)24 \qquad (2.14)$$

$$\sigma B'_i \zeta'_i = \frac{Q'_{i+1} - Q'_{i-1}}{\Delta x}; \quad i = 23(2)25, \qquad (2.15)$$

Equations (2.11, 12) and (2.14, 15) have the same form as (2.7, 8); note, however, that neither (2.12) nor (2.15) is applied to section 21. There, equation (2.13) expresses continuity of transport between the three regions and serves as the condition joining these regions, together with

$$\zeta_{21}(\text{Eastern}) = \zeta'_{21} = \zeta_{21}(\text{Central}) \qquad (2.16)$$

for profile continuity.

The procedure now is as follows. Starting with $\zeta_1 = 1.0$ ft (a convenient value) and an estimate for σ, we integrate (2.11, 12) stepwise to section $i = 21$, so that approximate values are obtained for ζ_i at $i = 3(2)21$ and for Q_i at

$i = 2(2)20$. In order to cross $i = 21$ and enter the Central Basin, equation (2.13) must be used to obtain Q_{22}. Since this equation involves Q'_{22}, we must first carry the integration into Long Point Bay for an approximation to Q'_{22}. To do so we note that at this stage the disturbance in Long Point Bay may be regarded as a co-oscillation with the imposed frequency σ and imposed elevation $\zeta'_{21} = \zeta_{21}$ at the mouth. In other words, with boundary condition $Q'_{26} = 0$ at the head, equations (2.14, 15) can be solved for ζ' and Q' in terms of $\zeta_{21} (= \zeta'_{21})$. The results can be written in continued-fraction form

$$
\begin{aligned}
Q'_{22} &= \left(\sigma c'_{22} + \left(\sigma d'_{23} + \left(\sigma c'_{24} + \left(\sigma d'_{25}\right)^{-1}\right)^{-1}\right)^{-1}\right)^{-1} \zeta_{21} \\
\zeta'_{23} &= \left(\sigma d'_{23} + \left(\sigma c'_{24} + \left(\sigma d'_{25}\right)^{-1}\right)^{-1}\right)^{-1} Q'_{22} \\
Q'_{24} &= \left(\sigma c'_{24} + \left(\sigma d'_{25}\right)^{-1}\right)^{-1} \zeta'_{23} \\
\zeta'_{25} &= \left(\sigma d'_{25}\right)^{-1} Q'_{24},
\end{aligned}
\qquad (2.17)
$$

where $c' \equiv \Delta x / g S'$ and $d' \equiv -\beta' \Delta x$. The first equation here is the only one needed at the present stage. With this expression for Q'_{22} in terms of ζ_{21}, equation (2.13) may be solved for Q_{22}. Returning to (2.11, 12), stepwise integration will

then bring us to Q_{80} , thus completing one cycle of the iterative procedure. Convergence to $Q_{80}=0$ is approached as usual by successive adjustment of σ . In this way satisfactory values are obtained for the frequency σ and for profile and transport in the main channel. The corresponding conditions in Long Point Bay may be determined then from (2.17)

In summary, the equations used for numerical integration are (2.17) for Long Point Bay, and

$$\zeta_{i+1} = \zeta_{i-1} - \sigma c_i Q_i \; ; \quad i = 2(2)78$$

$$Q_{i+1} = Q_{i-1} - \sigma d_i \zeta_i \; ; \quad i = 1(2)19, 23(2)79$$

$$Q_{22} = Q_{20} - \sigma d_{21} \zeta_{21} - Q'_{22}$$

for the main channel, where $c \equiv \Delta x/gS$ and $d \equiv -b\Delta x$. It should be added that since we have drawn curvilinear rather than the usual rectilinear sections (see figure 4), the section width b at ζ -sections was taken to be the area between neighboring Q -sections divided by Δx ; that is b_i (for odd i) is equal to the area between sections $i+1$ and $i-1$, divided by Δx .

3. Numerical results

Computed periods T_m of the first five modes of longitudinal free oscillations of Lake Erie are listed in column 1 of table 2. Also shown in this table (column 2) are the products $m \cdot T_m$, which for a rectangular basin of length L and uniform depth h are equal to the Merian period $2L/\sqrt{gh}$. If we take L equal to the length of the principal axis (figure 4), then $L = 40\,\Delta x = 40 \times 1/3 \times 10^5$ ft; with a mean depth $h = 60.7$ ft (table 1) and $g = 32.16$ ft sec^{-2}, we find a Merian period 16.8 hr. The ratios of $m T_m$ to 16.8 hr are given in column 3 of table 2. Thus, the first mode, with computed period 14.1 hr, is about 16 per cent faster than predicted by the Merian formula. The third- and fourth-mode periods are very close to their Merian values, while the second and fifth are slower than the Merian prediction. These differences are of course the result of departures of shape and bottom configuration of Lake Erie from that of a rectangle of uniform depth.

Comparison of the computed periods with observations will be made after assessment of corrections for earth's rotation, friction and other effects.

Figure 6 shows computed surface profiles (ζ) of the first

Table 2. Computed periods (T_m) of first five modes of longitudinal free oscillation of Lake Erie.*

Mode	1 T_m (hours)	2 $m \cdot T_m$ (hours)	3 $\frac{m \cdot T_m}{16.8}$
1	14.08	14.08	0.84
2	8.92	17.84	1.06
3	5.70	17.10	1.02
4	4.11	16.44	0.98
5	3.69	18.45	1.10

* See section 6 for corrections and comparison with observed periods.

five modes of longitudinal free oscillation of Lake Erie. All modes were assigned an amplitude of 1.0 ft at Buffalo. At Toledo, the computed amplitudes of the first and second modes are between 40 and 50 per cent greater than at Buffalo, the amplitude of the third mode is about the same as at Buffalo, and the amplitude of the fourth and fifth modes are about two-thirds that at Buffalo. The node of the principal mode lies on section 44, about 144 statute miles from Buffalo, whereas the midpoint of the axis is section 40, about 126 miles from Buffalo. Nodes of the third and fifth modes are clustered nearby: the third at section 49, the fifth at section 46. There is a similar cluster of nodes between sections 22 and 30.

An interesting aspect of the results shown in figure 6 is the co-oscillation of Long Point Bay, the profile of which is indicated by the short segments between sections 21 and 25. The free period of the Bay is approximately 2.5 hours (by numerical integration), so there is only slight excitation by the 14-hour oscillation (first mode). The second mode (9.1 hours) has a somewhat larger effect, but virtually no excitation is caused by the third mode (5.7 hours) because the latter has a node very close to the mouth of the Bay. However, there is very strong response to

the fourth mode (4.1 hours), and an approach to resonance with the fifth mode (3.7 hours).

Volume transport (Q) is shown in figure 7. The greatest transports (per foot of amplitude at Buffalo) occur in the central basin: 9×10^6 ft^3 sec^{-1} across section 44 by the first mode, 8×10^6 ft^3 sec^{-1} across section 28 by the second and 10×10^6 ft^3 sec^{-1} across section 48 by the third. These transports are roughly 40 times greater than the discharge of Lake Erie to the Niagara River.

The mean current speed $(u = Q/S)$ corresponding to the transports of figure 7 are shown in figure 8. The first mode has nearly uniform mean current of about 0.5 ft sec^{-1} (per foot of amplitude at Buffalo) throughout the central basin, except for a slight increase to 0.7 ft sec^{-1} at section 28, just west of Long Point. Near the western end of the central basin, there is a sharp increase to a peak current of 1.3 ft sec^{-1} at the Pelee Point constriction. The second mode shows an even greater peak current of 1.7 ft sec^{-1} at this section, owing to proximity of the node at section 65. Another interesting feature of figure 8 is the reduced currents in the eastern basin: just east of Long Point the values are about 0.2 ft sec^{-1}, the maximum currents in this basin being about 0.4 ft sec^{-1}.

4. Correction for earth's rotation

Effects of the earth's rotation can be included without difficulty in principle by formulating the problem in two space dimensions. However, despite proximity of the 14-hour period and the "inertia" period 17.8 hours (half pendulum day), there is close agreement between observed periods and those computed from the channel equations without rotation, as will be shown below. A plausible hypothesis to account for this fact is that the basin is too narrow to permit appreciable transverse motions to develop in response to Coriolis forces (dimensions of equivalent rectangle: about 1 to 6). One may infer then that the longitudinal oscillations are similar to Kelvin waves, in which Coriolis forces acting upon the longitudinal particle motion are balanced quasi-geostrophically by the pressure gradient associated with transverse slope of the surface profile. It is well known that in these circumstances the oscillation becomes amphidromic --- that is, the time of high water rotates (in a counterclockwise direction) around the basin --- while the period is unaffected.

Strictly speaking, exact geostrophic balance can be maintained in a progressive wave but not in a standing wave, because superposition of two oppositely moving progressive Kelvin waves

cannot produce a fixed surface of zero transport. Nevertheless, if one makes the working assumption that transverse accelerations are small, a good estimation of the transverse profile slope may be expected from the geostrophic relation

$$f\hat{u} = -g\,\partial\zeta^*/\partial y,$$

where $\hat{u}$ is the longitudinal particle speed calculated from the channel equations, ζ^* is the added surface displacement caused by the earth's rotation, and f is the Coriolis parameter, equal to 0.979×10^{-4} rad sec^{-1} at the mean latitude of Lake Erie. This procedure has been applied in numerous investigations of large, enclosed basins: for example, by Neumann (1942) for the Baltic, by F. Defant (1954) for Lake Michigan, and by Mortimer (1955) in connection with internal oscillations of Loch Ness.

The result of integrating the preceding equation across the channel may be written

$$\zeta_S^* - \zeta_N^* = -f b\,\hat{u}/g,$$

where subscripts S and N refer to the south and north shores of the section, and b is the section width. Assuming the geostrophic effect to be divided equally between the south and north shores, we have

$$\zeta_N^* = -\zeta_S^* = a\hat{Q} \qquad (4.1)$$

$$a \equiv f\ell/2gS$$

after substituting $\hat{u} = \hat{Q}/S$. (Note that the parameter a is a function of $\times$ which depends only upon the basin geometry.) It follows that <u>total</u> disturbances on south and north shores are $\hat{\zeta}_S = \hat{\zeta} - a\hat{Q}$ and $\hat{\zeta}_N = \hat{\zeta} + a\hat{Q}$, or after substitution of (2.3, 4) for $\hat{\zeta}, \hat{Q}$:

$$\hat{\zeta}_S = \zeta \cos\sigma t - aQ \sin\sigma t$$

$$\hat{\zeta}_N = \zeta \cos\sigma t + aQ \sin\sigma t \quad ,$$

where ζ, Q are the profile and transport solutions of the channel equations.

The preceding expressions are equivalent to

$$\hat{\zeta}_S = -A\cos\sigma(t - t_S) \qquad (4.2)$$

$$\hat{\zeta}_N = -A\cos\sigma(t - t_N) \quad ,$$

where the amplitude A and the times t_S, t_N of high water are given by

$$A = \sqrt{\zeta^2 + a^2 Q^2} \tag{4,3}$$

$$\left\{ \begin{aligned} t_S &= \sigma^{-1} \arccos(-\zeta/A) \\ &= \sigma^{-1} \arcsin(aQ/A) \end{aligned} \right\} \tag{4,4}$$

$$t_N = T - t_S \tag{4,5}$$

with $0 \leq t_S \leq T$ and $T \equiv 2\pi/\sigma$ the oscillation period.

In writing (4.2-5) the convention is made that $\zeta < 0$ at the western end of the basin (Toledo) for all modes. The phase of high water on the south shore then begins at zero at Toledo and increases to $\frac{1}{2}T$ at the end of the first amphidromic region. The results of calculations based upon (4.3, 4, 5) are given later.

The foregoing analysis is aimed at estimating the effect of the earth's rotation upon range and phase of oscillation. It is in general much more difficult to determine the effect of rotation upon the period of oscillation. For the reasons explained above, this effect apparently is not appreciable in the case of Lake Erie; but it is pertinent to attempt an assessment nevertheless. The problem one naturally is led to examine is that of a

rotating rectangular basin of uniform depth. This problem was attacked first by Rayleigh (1903, 1909), and subsequently was studied more rigorously by Taylor (1922), Lamb (1924, §212a), and others. The most recent investigations are those of Corkan and Doodson (1952) and, notably, of Van Dantzig and Lauwerier (1960).

For the purpose of the present discussion it is sufficient to quote a result given by Lamb (1924, §212a; see also 1932, §212a). Let L and b denote the length and breadth of a rectangular basin of uniform depth h, and let

$$\sigma_L \equiv \pi\sqrt{gh}/L \quad ; \quad \sigma_b \equiv \pi\sqrt{gh}/b$$

denote the frequencies of the lowest longitudinal and transverse modes without rotation. Lamb's result is that, provided the rotation is small (specifically, $f^2 \ll \sigma_L^2$), the frequency with rotation is given approximately by the biquadratic equation*

---

* Equation (4.6) is correct (to within order f^2) for a square basin; for a rectangular basin, the coefficient $64/\pi^4$ is an approximate value obtained by neglecting contributions from all but the lowest longitudinal and transverse modes.

$$(\sigma^2 - \sigma_L^2)(\sigma^2 - \sigma_f^2) = f^2\sigma^2 \cdot 64/\pi^4 \quad . \qquad (4.6)$$

From (4.6) one finds two frequencies, one of which is less than σ_L , the other greater than σ_f , as is shown clearly in figure 9. In this figure the left and right sides of (4.6) are graphed schematically as ordinates, with σ^2 as abscissa; intersections of the two curves give the roots of (4.6). From this result one infers that the period of the lowest longitudinal mode is <u>increased</u> by rotation, while that of the lowest transverse mode is decreased.

Analysis of the rotating rectangular basin is complicated in part because of the presence of corners; one might logically, therefore, seek an analysis of, say, an elliptic basin. In the nonrotating case, the elliptic basin of uniform depth has been considered by Jeffreys (1925) and Goldstein (1928), while Goldsbrough (1931) treated the elliptic paraboloid. In the rotating case, Goldstein (1929) treated the elliptic basin of uniform depth, for which he obtained numerical results for the lowest longitudinal and lowest transverse modes. By comparison of these results with those given in his discussion of the corres-

ponding nonrotating case (Goldstein, 1928), one finds that the period of the lowest longitudinal mode is increased by rotation.*

---

* It is not possible to infer from Goldstein's work a corresponding result for the lowest transverse mode.

Moreover, this mode is a "positive" wave; that is, the cotidal lines rotate in a counterclockwise direction (in other words, in the same sense as the rotation of the system). On the other hand, the lowest transverse mode is a "negative" wave, with clockwise rotation of cotidal lines. All of these features are qualitatively in accord with the results for a rotating rectangular basin.

The work cited above gives a clear indication that the period of the lowest longitudinal mode of Lake Erie is increased by rotation, but does not provide a convenient means for estimating the magnitude of this increase. The writers fortunately have had an opportunity to learn of work done recently by F. K. Ball, who kindly has permitted us to describe some of his remarkable results. Ball finds an <u>exact</u> solution in simple, closed form for the profile and frequency of the lowest longitudinal and transverse modes in the very interesting case of a rotating, elliptic parobo-

loid. To explain his result, we first write the equation for the law of depth:

$$h = 2\bar{h}\left(1 - \frac{4x^2}{L^2} - \frac{4y^2}{b^2}\right) ,$$

where $\bar{h}$ is the mean depth (the ratio of volume to surface area) and L, b are the lengths of the basin axes (twice the lengths of the semi-axes). In the nonrotating case, Ball obtains for the frequencies of the lowest longitudinal and lowest transverse modes

$$\sigma_L \equiv 4\sqrt{g\bar{h}}/L \quad ; \qquad \sigma_b \equiv 4\sqrt{g\bar{h}}/b ,$$

exactly (a result contained also in Goldsbrough's (1931) work). His solution for the corresponding frequencies in the rotating case is most remarkable: it is exactly of the form (4.6) without approximation and without any restriction as to the size of f (and with the coefficient $64/\pi^4$ on the right replaced by unity). It follows, as in the previous cases, that the period of the lowest longitudinal mode is increased (and that of the lowest transverse mode decreased) by rotation.* Moreover, if one solves this

---

* Ball also finds, as in the previous cases, that the

lowest longitudinal mode is a "positive" wave, the lowest transverse mode a "negative" wave.

---

equation for the period of the lowest longitudinal mode in the case $(\delta/L)^2 \ll 1$ which applies to Lake Erie, the result can be written

$$\frac{T}{T_L} = 1 + \frac{1}{2}\left(\frac{\delta}{L}\right)^2 \cdot \left(\frac{T}{T_i}\right)^2 + O\left(\frac{\delta}{L}\right)^4 , \qquad (4.7)$$

where $T_L \equiv 2\pi/\sigma_L$ is the period of the lowest longitudinal mode in the nonrotating case, and T_i is the "inertia" period $2\pi/f$.

For Lake Erie, δ/L = 0.20 gives an ellipse having the actual surface area (27.6×10^{10} ft^2 = 9,900 mi^2) and length (L = 250 miles); thus $(\delta/L)^2$ = 0.41 in (4.7). The observed T = 14.4 hr and T_i = 17.8 hr, so $(T/T_i)^2$ = 0.65. The second term in (4.7) therefore has the numerical value 0.013. In other words, Ball's result for the rotating elliptic paraboloid enables us to estimate that the period of the lowest longitudinal mode of Lake Erie is increased about 1.3 per cent by the earth's rotation.

The results described above suggest that in any rotating,

elongated basin the lowest longitudinal mode is a "positive" amphidromic wave with period greater than in the nonrotating case, while the lowest transverse mode is a "negative" amphidromic wave with period less than in the nonrotating case. If the basin is sufficiently elongated, the increase of period of the longitudinal mode is not more than a few per cent. Presumably, in the longitudinal mode the transverse profile slope is on the whole slightly super-geostrophic with respect to the longitudinal particle motion; the small, transverse accelerations which then act to the left of the longitudinal particle motion produce counterclockwise ("positive") rotation of the cotidal lines. The particle orbits are elliptical, the shorter axis being transverse to the basin; when projected in a horizontal plane the orbital motion is counterclockwise. Conversely, profile slopes are sub-geostrophic in the transverse mode, so rotation of cotidal lines is clockwise, and orbital motion is clockwise.

5. Corrections for friction, variation of mean lake level, and end effects

The fundamental difficulty in assessing effects of friction in a "geophysical" basin is that no procedure is known by which turbulent frictional forces can be introduced into the

differential momentum equations in a rigorous manner. Moreover, all heuristic procedures require the use of a friction parameter --- such as a skin-friction coefficient or an eddy viscosity --- the numerical value of which depends upon the physical state of the medium as well as upon the nature of the bottom surface and is unknown a priori. In general, therefore, the geophysical data must be used in the first instance as a basis for selecting an appropriate heuristic formalism for friction, and for assigning a numerical value to the corresponding parameter. On Lake Erie, the only reliable data available for this purpose are water-level records. A special study of these data could be aimed at establishing a law of friction for the basin as a whole; however, in the present work we have limited our investigation to the question: for a specified law of friction, what is the relation between period increase and decay modulus (natural logarithm of ratio of successive amplitudes)?

This question is pertinent simply because the decay modulus can be estimated, at least roughly, by direct examination of water-level records. Thus, Endrös (1934) gives 0.39 for the decay modulus of the lowest mode, while Hunt (1959) finds 0.86, Gillies (private communication) 0.85, and Platzman (1963) 0.65

to 0.70. It is possible that the disparity between the latter values and the small value 0.39 quoted by Endrös reflects an amplitude - dependence of decay modulus (a nonlinear effect); but whatever the explanation, it seems safe to say that typical values of decay modulus for the fundamental mode of Lake Erie are in the range 0.4 to 0.9.

If $\hat{\tau}$ denotes the horizontal shear stress, the momentum and mass equations can be written

$$\frac{\partial \hat{u}}{\partial t} = -g\frac{\partial \hat{\zeta}}{\partial x} + \frac{1}{\rho}\frac{\partial \hat{\tau}}{\partial z} \qquad (5.1)$$

$$\frac{\partial \hat{\zeta}}{\partial t} = -\frac{\partial}{\partial x}\int_{-h}^{0} \hat{u}\, dz \quad , \qquad (5.2)$$

where z is an upward vertical axis with origin in mean level of free surface. Integration over a section yields

$$\frac{\partial \hat{Q}}{\partial t} = -gS\frac{\partial \hat{\zeta}}{\partial x} - F b/\rho \qquad (5.3)$$

$$\frac{\partial \hat{\zeta}}{\partial t} = -\frac{1}{b}\frac{\partial \hat{Q}}{\partial x} \quad , \qquad (5.4)$$

where F is the mean bottom stress across the section. The most plausible assumption about F is the quadratic stress law $F_2 = k\rho|\hat{u}|\hat{u}$, where k is a skin-friction coefficient

(the value of which is found to be about 3×10^{-3} in work on tidal friction). However, with the use of F_2 the harmonic composition of each mode is distorted by "overtides." To avoid this complication one can adopt a linear stress law $F_1 \equiv k\rho\mathcal{U}\hat{u}$, where $\mathcal{U}$ is a constant velocity chosen so that the linear law simulates the quadratic as nearly as possible.

An alternative formulation is to adopt the Boussinesq hypothesis of a linear shear stress $\hat{\tau} = \mu \partial\hat{u}/\partial z$, where μ is a turbulent viscosity coefficient. This permits some insight into vertical structure of the disturbance. With the use of this expression for $\hat{\tau}$, Proudman and Doodson (1924) in a classical study have solved (5.1, 2) for oscillations in a rectangular basin of length L and uniform depth h, with a uniform value of eddy viscosity $\nu \equiv \mu/\rho$ and no slip at the bottom. They find a solution in the form of a damped harmonic oscillator:

$$\hat{\zeta} \sim e^{-pt} \cos qt \cos(\pi x/L),$$

in which decay rate p and frequency q depend upon external parameters through the dimensionless ratio

$$\alpha \equiv (p_0/q_0)^2 .$$

Here $p_0 \equiv \nu/h^2$ may be regarded as the decay rate associated with a viscous boundary layer of depth h, and $q_0 \equiv \pi\sqrt{gh}/L$ is the frequency of inviscid oscillations. Alternatively, $\delta \equiv \sqrt{\nu/q_0}$ may be regarded as the thickness of the boundary layer associated with a free flow that oscillates with frequency q_0, in which case $\alpha = (\delta/h)^4$. We shall refer to α as the "Proudman number."

Proudman and Doodson show that $p' \equiv p/p_0$ and $q' \equiv q/p_0$ are functions only of the Proudman number, and are determined by the transcendental equation

$$\tan\theta = \theta + \alpha\theta^5 \qquad (5.5)$$

$$\theta \equiv (p' + iq')^{1/2} .$$

If $\alpha < \alpha_c = 0.53667$, this equation has two conjugate complex roots (which give the oscillatory solution), and an infinite num-

ber of real roots (which give non-oscillatory solutions.) If $\alpha > \alpha_c$ all roots are real. Evidently, the critical Proudman number α_c corresponds to critical damping.

Restricting attention to the underdamped solution, we introduce in place of p the decay modulus

$$\beta \equiv pT = 2\pi p/q = 2\pi p'/q' \ ,$$

where T is the oscillation period; evidently $e^{-\beta}$ is the ratio of successive maxima of the solution. In place of q we introduce the period ratio

$$\gamma \equiv \frac{T}{T_0} = \frac{q_0}{q} = \frac{q_0}{q' p_0} = \frac{1}{q'\sqrt{\alpha}} \ ,$$

where T_0 is the period of inviscid oscillations. Since p' and q' are functions only of α, it is clear that the same is true of β and γ. The dependence of β and γ upon α in the range $0 < \alpha < \alpha_c$ is shown by the curves in figure 10, which have been obtained by numerical solution of (5.5). It is clear also that γ may be regarded as a function of β; this relation is shown in the range $0 < \beta < 1.2$ by the solid curve in figure 11. The latter gives one answer to the question originally posed, by showing the relation between period ratio and

decay modulus that results from the eddy viscosity formalism adopted in the work of Proudman and Doodson. It is important to note that while this relation depends upon the <u>form</u> of the law of friction adopted, it does not depend upon the numerical value of the friction parameter. Thus, the solid curve in figure 11 is independent of the numerical value of eddy viscosity.

Since $\alpha < 10^{-2}$ when $\beta < 1$, we see that $\alpha \ll 1$ in the range of β-values with which we are concerned. By analysis of (5.5) in the limit $\alpha \to 0$, it is possible to show that

$$\beta \; (= 2\pi p'/q') \longrightarrow \tfrac{1}{2}\pi \cdot (4\alpha)^{\frac{1}{4}}$$
$$\gamma \; (= 1/q'\sqrt{\alpha}) \longrightarrow 1 + \tfrac{1}{4}(4\alpha)^{\frac{1}{4}}, \qquad (5.6)$$

from which it follows that

$$\gamma = 1 + (\beta/2\pi) + O(\beta^2). \qquad (5.7)$$

Thus, $\gamma = 1 + O(\beta)$ in the limit $\beta \to 0$. It is interesting to note that the expression for β in (5.6) can be shown to be equivalent to a result given by Keulegan (1959), who calculated the decay modulus of standing waves in rectangular basins, by

evaluation of energy dissipation in the boundary layers. In the present notation, Keulegan's equation (23) can be written

$$\beta = \tfrac{1}{2}\pi C \cdot (4\alpha)^{\frac{1}{4}} \qquad (5.8)$$

$$C = 2\left(\frac{h}{\ell} + \frac{h}{L}\right) + \frac{2\pi h}{L}\left(1 - \frac{2h}{L}\right)\Big/ \sinh \frac{2\pi h}{L} .$$

The factor C depends only upon the dimensions of the basin. For a "geophysical" basin, where $h \ll \ell$ and $h \ll L$, it is easy to see that $C \approx 1$, in which case (5.8) and (5.6) give the same β. It should also be remarked that Keulegan's measurements of decay of standing waves in laboratory basins were in good agreement with the form of relation given in (5.8). (These measurements were in the range $\beta < 0.2$.)

In the case of linear friction, (5.3) becomes

$$\frac{\partial \hat{Q}}{\partial t} = -gS \frac{\partial \hat{\zeta}}{\partial x} - k u \frac{b}{S} \hat{Q} . \qquad (5.9)$$

Assume now a harmonic solution

$$\hat{Q} = \mathrm{Im}\, Q(x)\, e^{i\sigma t}$$

$$\hat{\zeta} = \mathrm{Re}\, \zeta(x)\, e^{i\sigma t} \qquad (5.10)$$

where Q, ζ and σ are in general complex. Substitution in (5.4) and (5.9) gives

$$\sigma\zeta = \frac{1}{B}\frac{\partial Q}{\partial x} \qquad (5.11a)$$

$$\sigma Q = -gS\frac{\partial \zeta}{\partial x} + ik\mathcal{U}\frac{B}{S}Q \ . \qquad (5.11b)$$

For a rectangular basin of length L and uniform depth h, these equations have constant coefficients and give damped simple-harmonic oscillations with $\sigma = ip \pm q$, the decay rate p and frequency q being given by

$$p = k\mathcal{U}/2h \quad ; \quad q = \sqrt{q_0^2 - p^2} \qquad (5.12)$$

(where $q_0 \equiv \pi\sqrt{gh}/L$), as is easily verified. Hence $q_0 = \sqrt{q^2+p^2}$, so we get through division by q:

$$\gamma = \sqrt{1+(\beta/2\pi)^2} \ , \qquad (5.13)$$

where $\gamma = q_0/q$ is the period ratio and $\beta = 2\pi p/q$ the decay modulus. Equation (5.13) gives the relation between β and γ for any damped, simple-harmonic oscillator. This relation is shown by the broken curve in figure 11. It should be

noted that in contrast to (5.7), we have

$$\gamma = 1 + \tfrac{1}{2}(\beta/2\pi)^2 + O(\beta^4)$$

from (5.13). Thus, $\gamma = 1 + O(\beta^2)$ in the limit $\beta \to 0$ for linear friction.

For a general channel, when the coefficients b and S are functions of x, equations (5.11) may be integrated numerically if a numerical value is assigned to $k\mathcal{U}$. However, since the oscillations of Lake Erie are not strongly damped, one may regard the friction term in (5.11) as a small term, and by a perturbation analysis seek its modification of the solution without friction. This analysis proceeds by expansion of σ in powers of $ik\mathcal{U}$:

$$\sigma = \sigma_0 + \sigma_1 \cdot (ik\mathcal{U}) + \sigma_2 \cdot (ik\mathcal{U})^2 + \ldots, \quad (5.14)$$

and similar expansions for ζ and Q. Development of (5.11) in powers of $ik\mathcal{U}$ leads to pairs of equations for successive determination of ζ_0, Q_0; ζ_1, Q_1 ...., together with σ_0, σ_1 ... for frequency. The results of this analysis can be stated most readily in terms of perturbations of the integrals

$$K \equiv \tfrac{1}{2}\int_0^L \frac{Q^2}{S}\,dx \quad ; \quad W \equiv \tfrac{1}{2}\int \frac{Q^2}{S^2}\,f\,dx \,.$$

To the lowest order, ρK is the total kinetic energy and $\rho k^2 u W$ the dissipation rate for the basin as a whole.

The first result of the perturbation analysis is*

---

* Equation (5.15) is derived in appendix A.

$$\sigma_1 = \tfrac{1}{2} W_0 / K_0 \,, \qquad (5.15)$$

which determines the first-order perturbation of σ in terms of integrals that involve only the ground state. Since σ_1 is real, (5.14) shows that to the first order, friction does not modify the period, but introduces a decay at the rate $p = k u \sigma_1$. The corresponding decay modulus is

$$\beta = 2\pi p/\sigma_0 = 2\pi k u \sigma_1 / \sigma_0 \,. \qquad (5.16)$$

For a rectangular basin it is easy to see that (5.15) gives $\sigma_1 = 1/2h$, so we recover the result stated for p in (5.12).

The next stage of the perturbation analysis gives*

---

* Equation (5.17) is derived in appendix A.

$$\sigma_2 = \frac{1}{2}\frac{\sigma_1^2}{\sigma_0} + \frac{1}{4}\frac{W_1 K_0 - W_0 K_1}{K_0^2} , \qquad (5.17)$$

which determines σ_2 in terms of integrals that involve the ground state and the first-order perturbation Q_1. The latter enters through

$$K_1 = \int_0^L \frac{Q_0 Q_1}{S} dx \; ; \quad W_1 = \int_0^L \frac{Q_0 Q_1}{S^2} f\, dx .$$

Since σ_2 is real, (5.14) shows that the second-order effect of friction does not alter the decay rate, but modifies the frequency. If the frequency is denoted $q \equiv \mathrm{Re}\,\sigma$, we have from (5.14):

$$q = \sigma_0 - \sigma_2 \cdot (k\mathcal{U})^2 + O(k^4) ,$$

so the period ratio is

$$\gamma = \frac{\sigma_0}{q} = 1 + (k\mathcal{U})^2 \cdot \frac{\sigma_2}{\sigma_0} + O(k^4) . \qquad (5.18)$$

If $k^2 U$ is stated in terms of the decay modulus through (5.16), and (5.17) is used for σ_2 , we have

$$\gamma = 1 + B \cdot (\beta/2\pi)^2 + O(\beta^4) \qquad (5.19)$$

$$B \equiv \frac{\sigma_2 \sigma_0}{\sigma_1^2} = \frac{1}{2} + \frac{\sigma_0 (W_1 K_0 - W_0 K_1)}{W_0^2} .$$

Equation (5.19) expresses the period ratio through terms of second order in the decay modulus, for an arbitrary channel with linear friction. For a rectangular basin one finds $Q_1 = 0$ so $K_1 = 0 = W_1$ and $B = \frac{1}{2}$; then (5.19) becomes equivalent to (5.13) to the second order.

Equation (5.19) is of interest as showing that the effect of channel configuration on the β, γ relation can be formulated in a straightforward and explicit manner. Numerical computations for the lowest mode of Lake Erie yielded the following results:

$$\begin{aligned} K_0 &= 0.192 \times 10^{13} \text{ ft}^5 \text{ sec}^{-2} \\ W_0 &= 0.396 \times 10^{11} \text{ ft}^4 \text{ sec}^{-2} \\ K_1 &= -0.309 \times 10^{14} \text{ ft}^4 \text{ sec}^{-1} \\ W_1 &= -0.174 \times 10^{13} \text{ ft}^3 \text{ sec}^{-1} \end{aligned} \qquad (5.20)$$

from which (5.15) and (5.19) give $\sigma_1 = 0.0103 \text{ ft}^{-1}$. (With this value of σ_1 and a skin-friction coefficient $k = 0.0025$, the

modulus (5.16) becomes $\beta = 1.3\,\mathcal{U}$ when $\mathcal{U}$ is expressed in ft sec^{-1}. Thus, a decay modulus of 0.65 would correspond to $\mathcal{U} = 0.5$ ft sec^{-1}, not an unreasonable value in light of the results shown in figure 8.) From the numerical data in (5.20), we find that in (5.19) the coefficient $B = 0.330$. The corresponding curve of γ versus β is shown in figure 11 as a dotted line.

The conclusions that may be drawn from the foregoing discussion are as follows. If one considers friction to act in the manner of a laminar boundary layer, the analysis of Proudman and Doodson (1924) may be used to show that the period is increased by about 9 per cent for a decay modulus of 0.7 (figure 11). If resistance is better represented by a linear skin-friction law, the increase of period is less than 1 per cent for a decay modulus of 0.7. The latter estimate takes into account actual basin configuration, while the former is derived from the model of a rectangular basin of uniform depth. The matter actually is further complicated by the earth's rotation (see Platzman, 1963).

Next, we turn briefly to consider the correction for variation of mean lake level. The bathymetric chart used to establish areas of vertical sections is based upon a mean lake

level of 568.6 ft MSL-IGLD*, which is a low-water reference for

* International Great Lakes Datum of 1955.

Lake Erie. There are however, annual and secular variations of mean lake level that are accompanied by corresponding small variations of section area. Thus, if δh denotes a small variation of mean lake level, the corresponding variation of section area is $\delta S_i = b_i \, \delta h$, which causes a variation in the coefficient S of (2.5). The effect that these small variations have on the computed periods may be assessed by perturbation analysis of (5.11) --- without the friction term --- beginning with expansion of σ in powers of δh :

$$\sigma = \sigma_0 + \sigma_1 \cdot (\delta h) + \sigma_2 \cdot (\delta h)^2 + \cdots$$

The first-order effect is easily found to be*

* Equation (5.23) is derived in appendix B.

$$\sigma_1 = \sigma_0 \cdot \tfrac{1}{2} W_0 / K_0 \, . \qquad (5.23)$$

The corresponding period ratio evidently is $\gamma = \sigma_0/(\sigma_0+\sigma_1\delta h)$, or

$$\gamma = 1 - (\tfrac{1}{2}W_0/K_0)\cdot\delta h + O(\delta h)^2. \qquad (5,24)$$

Numerical values of K_0 and W_0 for the lowest mode are given in (5.20), from which we find $\frac{1}{2}W_0/K_0 = 0.0103$ ft^{-1}. It follows from (5.24) that for the lowest mode, the period correction for mean lake level is equal very neraly to $-\delta h$ per cent if δh is expressed in feet.

Finally, we consider correction for the effect of inflow and outflow channels at the ends of the basin. The quasi-steady flow of about 200,000 ft^3 sec^{-1} through the basin from west to east cannot have any effect upon oscillations calculated from the linearized channel equations, but there are <u>variations</u> of inflow and outflow caused by the variations of lake level that accompany free oscillations. Thus, a change of 1.0 ft in lake level at Buffalo produces a change of about 20,000 ft^3 sec^{-1} in discharge to the Niagara River, the principal outflow channel. This coupling of the oscillations with inflow and outflow has an effect similar to that of friction. Since the peak trans-

port associated with the oscillation itself is about 10^7 ft^3 sec^{-1} (figure 7) --- that is, about 500 times greater than discharge variations at the ends of the basin --- it is clear that the problem can be investigated by means of a perturbation analysis.

Let λ be the discharge variation per foot of lake-level variation at the head of the outflow channel (Niagara River), and μ the corresponding quantity for the mouth of the inflow channel (Detroit River), so the end conditions are

$$\text{at } x=0 \text{ (inflow end)}: \quad \hat{Q} = -\lambda\hat{\zeta}$$
$$\text{at } x=L \text{ (outflow end)}: \quad \hat{Q} = +\mu\hat{\zeta},$$

the signs being chosen to make λ and μ positive. (Note that the positive direction of $\hat{Q}$ is taken as opposite to the direction of flow-through.) Since our equations are linear, we may consider each end separately; assume therefore that the inflow end is closed $(\mu=0)$ and the outflow end open. In terms of the representations (5.10) these boundary conditions are

$$\begin{aligned} x=0: &\quad Q = -i\lambda\zeta \\ x=L: &\quad Q = 0 \,. \end{aligned} \tag{5.25}$$

Starting again from the basic equations (5.11), but without the friction term, we expand in powers of $i\lambda$; thus

$$\sigma = \sigma_0 + \sigma_1 \cdot (i\lambda) + \sigma_2 \cdot (i\lambda)^2 + \ldots$$

The first-order effect is found to be*

---

* Equation (5.26) is derived in appendix C.

$$\sigma_1 = \tfrac{1}{2} Z_0 / K_0 \qquad (5.26)$$

$$Z_0 \equiv \tfrac{1}{2} g (\zeta^2)_{x=0} ,$$

so there is a decay at the rate $p = \lambda \sigma_1$, with modulus

$$\beta = 2\pi p / \sigma_0 = \lambda \sigma_1 T_0 . \qquad (5.27)$$

Since the amplitude at Buffalo is taken to be 1.0 ft in our computations, we have $Z_0 = \tfrac{1}{2} g (\zeta_0^2)_{x=0} = 16.1$ ft^3 sec^{-2}; with K_0 as in (5.20), this makes $\sigma_1 = 0.20 \times 10^{-11}$ ft^{-2}. Using $T_0 = 14.1$ hr and $\lambda = 20{,}000$ ft^3 sec^{-1} ft^{-1}, (5.27) gives

β = 0.002 for the decay modulus imposed by the outflow channel. Even after inclusion of a contribution from the inflow channel, the decay modulus associated with open ends is not likely to exceed 0.01 --- a value about 50 times smaller than that produced by friction. The effect of open ends on the period therefore may be considered to be negligible.

6. Verification analysis

Owing to the very strong response of Lake Erie to wind action, verification of the results shown in figures 6, 7 and 8 should be based upon statistical analysis of a fairly large mass of data. For currents, such data do not exist; but fortunately, continuous water-level recording gages have been maintained on the Great Lakes for many years by the U. S. Lake Survey and by the Canadian Hydrographic Service. The writers have analyzed covariance spectra of these records for data available at 13 stations (locations of which are shown in figure 4) during the six-month period 1 April 1958 through 30 September 1958. The details of this work are given elsewhere (Platzman and Rao, 1963). Here it suffices to note that spectral analysis was made at each station with lag resolution one hour and frequency resolution 0.1 cycle per day. In these analyses, very distinct peaks were found

at a frequency 1.70 cpd (period 14.12 hr), and at other frequencies that correspond well with the higher modes of oscillation, as will be discussed in detail later. Analyses at several stations were made with frequency resolution 0.05 cpd; these gave a consistent peak variance at 1.65 cpd (14.55 hr).

Accordingly, in the analyses at resolution 0.1 cpd the sum of spectral amplitudes at 1.60 and 1.70 cpd was taken to determine the amplitude of the fundamental mode; this sum multiplied by 0.1 cpd gives the variance contribution in the frequency band 1.55 cpd (15.48 hr) to 1.75 cpd (13.71 hr). If the quantity thus obtained is denoted V, then $\sqrt{V}$ may be regarded as proportional to an estimate of the observed amplitude of the fundamental mode. Since computed amplitudes are based upon the arbitrary value 1.0 ft at Buffalo, the ratio $\sqrt{V/V_B}$ x 1.0 ft has been defined as the "observed" amplitude relative to that at Buffalo, where V_B is the value of V at Buffalo.

Comparison between computed and observed amplitudes is shown in figure 12, where the solid curve is the computed amplitude from (4.3). (The broken curve is computed amplitude without allowance for earth's rotation, and is the same as the absolute value of the corresponding curve in figure 6.) Figure 13 shows a

similar comparison for the second mode, in which the frequency band 2.55 to 2.75 cpd was used to estimate the observed amplitude. In spite of uncertainties in the spectral analysis, agreement between computed and observed amplitudes may be considered on the whole satisfactory. (At Port Clinton, Port Dover and Fairport the hourly records covered only about 4 months in the 6-month period selected for analysis, so the spectral estimates there are less reliable than at other stations. Port Clinton, especially, shows poor agreement in figures 12 and 13.)

It is also possible to use the covariance spectra to infer relative amplitudes of various modes at individual stations. Table 4 shows the results for the first four modes at Toledo and Buffalo. Columns 2 and 4 give the contribution V_m to variance in the frequency bands listed in column 1 (each of which is centered on the frequency giving (locally) maximum response, and is 0.2 cpd in width). Column 3 gives estimates for Toledo of the amplitude of modes 2, 3 and 4 relative to mode 1; column 5 gives relative amplitudes at Buffalo. There is good agreement between Toledo and Buffalo for relative amplitudes of second and third modes. The enhancement of mode 4 at Buffalo (period about 4 hours) may be the result of oscillations involving Long Point Bay.

TABLE 4. Spectral estimates of variance V_m and relative amplitude $\sqrt{V_m/V_1}$ of first four modes at Toledo and Buffalo.

1		2	3	4	5
		Toledo		Buffalo	
Mode m	Frequency band (cpd)	V_m ($ft^2 \times 10^4$)	$\sqrt{\frac{V_m}{V_1}}$	V_m ($ft^2 \times 10^4$)	$\sqrt{\frac{V_m}{V_1}}$
1	1.55 - 1.75	218	1.00	109	1.00
2	2.55 - 2.75	26.0	0.35	14.3	0.36
3	3.95 - 4.15	7.91	0.19	5.30	0.22
4	5.65 - 5.85	3.32	0.12	8.44	0.28

Turning now to the phase, figures 14 and 15 show results obtained for the first and second modes. The solid curve gives phases t_S, t_N of high water on the south and north shores of the Lake, computed from (4.4, 5), on the convention that $t_S = 0$ at Toledo. The broken curve gives phases that would be obtained without earth's rotation, from which it is evident that rotation has a marked effect, particularly upon the first mode; thus, near the node of the first mode, the phase differs by more than 3 hr from what it would be in absence of rotation.

The observed phases, shown by dots in figures 14 and 15, were obtained from cross-spectral anlyses between Toledo and each of the other stations. Coherences for these station pairs are uniformly high, with a few exceptions such as Fairport in the first mode and Huron in the second.* Verification of phases in the first

---

* Six months of record were analyzed at most stations. At Fairport and Huron only four months were available. The relatively low coherence obtained at these stations may be ascribed to this deficiency and to the fact that Fairport is near the node of the first mode, while Huron is near a node of the second.

---

mode is on the whole satisfactory. In deciding whether the data reveal an amphidromic effect of the earth's rotation on the first mode, the records at Cleveland, Fairport and Port Stanley are crucial, owing to proximity of these stations to the node. At Cleveland, where the phase difference produced by rotation is about 1.1 hr, agreement between computed and observed phases is excellent. Similarly, at Port Stanley the spectral analysis gives a phase lag of 2.6 hr with respect to Buffalo, which qualitatively is in good accord with the behavior of an amphidromic wave.

There is one discrepancy between computed and observed phases that is worth noting. At Buffalo, and also at nearby Port Colborne, the phases obtained from spectral analysis are about 6.3 hr (relative to Toledo) at 1.70 cpd; in other words, in the wave of 1.70 cpd frequency, 6.3 hr are required for high water to travel along the south shore from Toledo to Buffalo. Since the period that corresponds to 1.70 cpd is 14.1 hr, it follows that in this wave 7.8 hr are required for high water to travel along the north shore from Buffalo to Toledo. Thus, the spectral analyses indicate that for the lowest mode, the travel time of high water from one end of the basin to the other is 1.5 hr

longer in westward movement along the north shore than in eastward movement along the south shore. This asymmetry cannot be accounted for theoretically in any reasonable way within the confines of the channel approximation, and may be regarded as evidence that completely satisfactory agreement between computed and observed properties of free oscillations can be obtained only from a two-dimensional model.

Table 5 presents a verification analysis of the periods of the first five modes of longitudinal free oscillation of Lake Erie. Column 1 gives the computed period from table 2; that is, the period resulting from numerical integration of the channel equations, by the method outlined in section 2. For the purpose of establishing statistically meaningful values of observed free periods as a basis for comparison with those computed theoretically, the writers analyzed covariance spectra of water levels at Toledo, Cleveland, Buffalo, and Port Stanley (for the six-month period 1 April 1958 through 30 September 1958) with frequency resolution 0.05 cycles per day. At 1.65 cpd (14.55 hr) this gives a period resolution of about 0.5 hr; for the higher modes the resolution is less (i.e., better) than 0.2 hr. Very distinct peaks for the first four modes appear in these spectra, a typical

TABLE 5. Periods of the first five modes of longitudinal free oscillation of Lake Erie.

1	2	3	4	5
Mode	Computed period (hours)	Observed period (hours)	Error in computed period (hours)	Error in computed period (per cent)
1	14.08	14.38	-0.30	-2.1
2	8.92	9.14	-0.22	-2.4
3	5.70	5.93	-0.23	-3.9
4	4.11	4.15	-0.04	-1.0
5	3.69	?	?	?

example of which is shown in figure 16. From the shapes of these peaks the cirtical frequencies were estimated and averages taken for the four stations mentioned above. The corresponding periods are the values listed in column 3 of table 5.* Errors in the computed period are shown in columns 4 and 5.

* A satisfactory determination of the observed fifth-mode period could not be made because of proximity of this period to the noise level of the spectra.

Any attempt to account for the small errors shown in table 5 must deal with the following factors: (1) the earth's rotation, (2) friction, (3) mean lake level, (4) the channel approximation, and (5) truncation errors. In section 4, an estimate was made that the earth's rotation increases the period of the lowest longitudinal mode of Lake Erie by about 1.3 per cent. Fortuitously, this increase is cancelled by the correction for mean lake level, which in section 5 was shown to change the period of the lowest mode by very nearly $-\delta R$ per cent, where δR (in feet) is the variation of mean lake level relative to the reference plane 568.6 MSL-IGLD on the chart used to establish section data

for numerical integration. Since the observed periods in column 3 of table 5 are derived from lake-level data for summer 1958, when mean lake level was 569.9 ft MSL-IGLD, it follows that δh = 1.3 ft. This increase in mean lake level therefore reduces the period by 1.3 per cent.

In the preceding section it was shown that friction is not likely to increase the lowest-mode period by more than 9 per cent. Although the actual increase probably is very much smaller than this, possibly less than 1 per cent, the writers have not succeeded in arriving at a reliable estimate. It is clear, however, that the errors in column 5 are all negative, and therefore have the proper sign for reduction by correction for friction. The truncation errors are not difficult to estimate. One way to do so would be to repeat the numerical integration with (say) double the number of sections. Instead, we have the results of an integration in which the locations and number of sections were not changed, but Q-sections were placed on i = 1(2)79 and ζ-sections on i = 2(2)78. This means that what formerly were ζ-sections are now Q-sections and vice-versa. The resulting periods are about 1 per cent smaller than those in column 2 of table 5.

It is difficult to assess errors inherent in the channel approximation without recourse to a solution of the problem in two space dimensions. Some information was gained by altering the treatment of Long Point Bay: in particular, a calculation was made in which the mouth of the Bay was regarded as a rigid barrier, by taking $Q'_{22} = 0$ in (2.13). The periods found in this way are about 1 percent smaller than those in column 2 of table 5. Although Long Point Bay is not the only important deviation of basin geometry from that of a channel of gradually varying section, one can infer that the channel approximation contributes errors of about the same magnitude as those previously discussed, namely at most a few per cent. This inference is supported by Jeffreys' (1925) comparison of the period in an elliptic basin of uniform depth, with the period obtained from the corresponding channel equations; and especially by the numerous similar comparisons given many years ago by Hidaka (1931), in the first of a series of remarkable papers on oscillations in various types of basins and canals.

The general conclusion that seems appropriate in regard to verification of periods is that errors in the "raw" periods definitely are small enough to be caused by known effects for which adequate provision has not been made in this study, mainly two-dimensionality, the earth's rotation, and friction.

7. Summary

The first five modes of longitudinal free oscillation of Lake Erie have been investigated by numerical integration of the classical channel equations. Corrections are estimated for earth's rotation and for friction, as well as for effect of variation of mean lake level and of inflow and outflow channels. The earth's rotation increases the period of the lowest longitudinal mode by about 1.3 per cent and transforms this mode into an amphidromic wave with counterclockwise rotation of cotidal lines. Friction increases the period by at most a few per cent. Variation of mean lake level decreases the period by about 1 per cent per foot of rise in level; however, effect of inflow and outflow channels on the free oscillations is negligible.

Covariance spectra of lake level are used as a basis for verification of computed wave characteristics. These spectra show distinct peaks at the frequencies of free oscillation, from which amplitude and period can be estimated; phase is estimated from cross-spectra. Agreement between computed and observed wave characteristics is on the whole satisfactory. In particular, computed periods of the first three modes are 14.1, 8.9 and 5.7 hr; observed periods are 14.4, 9.1 and 5.9 hr. Somewhat better agree-

ment should be possible with computations based upon a two-dimensional model.

8. History

A short summary of past work on determination of the period of the lowest mode of oscillation of Lake Erie will be presented here.* The numerical results obtained by various authors are presented in table 6.

* For extensive information and bibliography on currents and oscillations of Lake Erie, the reader should consult Olson (1950) and Verber (1960).

One of the earliest attempts to determine the free period of the uninodal longitudinal oscillation of Lake Erie seems to have been made by Henry (1902). Using Merian's formula $2L/\sqrt{gh}$ for the period of the fundamental mode of oscillation in a non-rotating rectangular basin of length L and uniform depth h, Henry obtained a value of 18.0 hours, which differs considerably from the observed 14-hour period. Part of this large discrepancy between the observed and computed periods may be ascribed to his use of a value 50 ft for the depth, about 10 ft smaller

TABLE 6. Period values obtained by past investigators.

Author	Basin length (statute miles)	Basin mean depth (feet)	Computed period (hours)	Observed period (hours)
Henry (1902)	246	50	18.0	14
Endrös (1908)	245	*	17.2	14.3 12.65 16.4
Hayford (1922)	?	?	13.1	13.1
Whipple (1927)	?	?	14.4	14-16
Hunt (1959)	246	66	15.7	15
Green (1960)	-	-	-	14.1

* Endrös applied the Duboys formula, in which 55 m (180 ft) was used as the maximum depth.

than the actual one.

Endrös (1908) analyzed the limnograms presented by Henry to derive the observed values given in table 6. His computed value was found by the DuBoys method, in which the period is taken as $2\int_0^L (gh)^{-\frac{1}{2}} dx$. The 12.65-hour observed period was considered by Endrös to be due partly to tidal effects. Presumably, the proximity of this period to that of the uninodal longitudinal oscillation produces an interference, thus preventing either of the oscillations from continuing through many successive cycles (Darwin, 1911, p. 56). Endrös also detected a period of 8.8 hours (in Henry's limnograms), which he ascribed to the second harmonic of the longitudinal oscillations.

Hayford (1922) obtained an observed period of 13.1 hours through a process of averaging the periods of a large number of oscillations, after eliminating wind and barometric effects from the data. He also produced a theoretical value of 13.1 hours, by a DuBoys-type calculation applied to mean depths in the central and eastern basins. (Hayford does not give an explicit statement of his procedure; but it is clear that he excluded the western basin.) A period of 3.7 hours was observed by Hayford for the primary oscillation in the eastern basin alone. This could also be due to the

fifth harmonic of the longitudinal oscillation, as pointed out by Hutchinson (1957) and substantiated by our calculations (table 2). The observed period of the uninodal transverse oscillation is given as 2.6 hours by Hayford.

The computed periods given by Whipple (1927) and Hunt (1959) are based upon the use of Merian's formula. Green (1960) obtained the observed value of 14.1 hours by averaging the periods of 180 oscillations. One interesting feature noted by Green is the fact that there is a phase difference of about three hours between the times of high water at Buffalo and Port Stanley. Similar evidence of phase differences associated with the fundamental mode was given by Verber (1960), who discussed rotation of the nodal line. As shown in the present study, phase differences are a consequence of the fact that longitudinal oscillations of Lake Erie are in the nature of Kelvin waves which produce a counter-clockwise rotation of the cotidal lines.

Acknowledgments

The writers gratefully acknowledge assitance from Judith L. Thieleker, who programmed for high-speed computer all computations reported in this study. Water-level records used to derive covariance spectra were provided by the U. S. Lake Survey and by the Canadian Hydrographic Service.

APPENDIX

A. Derivation of (5.15) and (5.17)

The first step in the perturbation analysis of (5.11) is to form an "energy" integral: multiply (5.11a) by $-\frac{1}{2}gb\zeta$ and (5.11b) by $\frac{1}{2}Q/S$, add the resulting equations and integrate over the entire basin. If the end conditions are $Q = 0$, the result can be written

$$\sigma(K-P) = ik\mathcal{U}\cdot W \qquad (A.1)$$

$$K \equiv \frac{1}{2}\int_0^L \frac{Q^2}{S}dx$$

$$P \equiv \frac{1}{2}\int_0^L g\zeta^2 b\,dx$$

$$W \equiv \frac{1}{2}\int_0^L \frac{Q^2}{S^2}b\,dx \quad .$$

Now introduce expansions in powers of $ik\mathcal{U}$ as in (5.14). Development of (A.1) through second-order terms yields

$$K_0 - P_0 = \qquad (A.2a)$$

$$\sigma_0(K_1 - P_1) = W_0 \qquad (A.2b)$$

$$\sigma_0(K_2 - P_2) + \sigma_1(K_1 - P_1) = W_1 \quad , \qquad (A.2c)$$

where subscripts 0, 1, 2 are used in the sense of (5.14); thus

$$K_1 = \int_0^L \frac{Q_0 Q_1}{S}\,dx \;; \quad W_1 = \int_0^L \frac{Q_0 Q_1}{S^2}\,b\,dx, \tag{A.3}$$

and so on. Next expand (5.11) through second order:

$$\left\{ \begin{aligned} \sigma_0 \zeta_0 &= \frac{1}{b}\frac{\partial Q_0}{\partial x} \\ \sigma_0 Q_0 &= -gS\frac{\partial \zeta_0}{\partial x} \end{aligned} \right\} \tag{0a, 0b}$$

$$\left\{ \begin{aligned} \sigma_1 \zeta_0 + \sigma_0 \zeta_1 &= \frac{1}{b}\frac{\partial Q_1}{\partial x} \\ \sigma_1 Q_0 + \sigma_0 Q_1 &= -gS\frac{\partial \zeta_1}{\partial x} + \frac{b}{S}Q_0 \end{aligned} \right\} \tag{1a, 1b}$$

$$\left\{ \begin{aligned} \sigma_2 \zeta_0 + \sigma_1 \zeta_1 + \sigma_0 \zeta_2 &= \frac{1}{b}\frac{\partial Q_2}{\partial x} \\ \sigma_2 Q_0 + \sigma_1 Q_1 + \sigma_0 Q_2 &= -gS\frac{\partial \zeta_2}{\partial x} + \frac{b}{S}Q_1 \end{aligned} \right\} \tag{2a, 2b}$$

Multiply (1a) by $\frac{1}{2}gb\zeta_0$ and (0b) by $-\frac{1}{2}Q_1/S$; add and integrate:

$$\sigma_1 P_0 + \tfrac{1}{2}\sigma_0 (P_1 - K_1) = 0 \,. \tag{A.4}$$

Solving for σ_1 and using (A.2a, b), we get (5.15) directly.

Multiply (2a) by $\frac{1}{2}gb\zeta_0$ and (0b) by $-\frac{1}{2}Q_2/S$;

add and integrate. Also, multiply (1a) by $\frac{1}{4}gb\zeta_1$ and (1b) by $-\frac{1}{4}Q_1/S$; add and integrate. The sum of the two equations thus obtained is

$$\sigma_2 P_0 + \tfrac{1}{2}\sigma_1 P_1 + \tfrac{1}{4}\sigma_1(P_1-K_1) + \tfrac{1}{2}\sigma_0(P_2-K_2) = -\tfrac{1}{4}W_1 ,$$

or, in view of (A.2c),

$$\sigma_2 P_0 + \tfrac{1}{4}\sigma_1(P_1+K_1) = \tfrac{1}{4}W_1 .$$

Replacing $P_0 = K_0$ from (A.2a) and $P_1 = K_1 - W_0/\sigma_0$ from (A.2b), we get σ_2 as in (5.17).

To evaluate σ_2 , it is necessary to solve the first-order equations (1a, b) for Q_1 , which enters in the determination of K_1 and W_1 from (A.3). Equations (1a, b) state an inhomogeneous boundary-value problem. When σ_0, ζ_0, Q_0 correspond to the lowest mode, we solve this problem by the algorithm

$$\sigma_1\zeta_0 + \sigma_0\zeta_1^{(n)} = \frac{1}{b}\frac{\partial Q_1^{(n+1)}}{\partial x} \qquad (A.5a)$$

$$\sigma_1 Q_0 + \sigma_0 Q_1^{(n)} = -gS\frac{\partial \zeta_1^{(n+1)}}{\partial x} + \frac{b}{S}Q_0 , \qquad (A.5b)$$

where $\zeta_1^{(n)}, Q_1^{(n)}$ are the nth approximations to ζ_1, Q_1. An appropriate first approximation is $Q_1^{(1)} = 0$, since this is an exact solution when the channel is rectangular, as is easily verified.* Then (A.5b) is integrated for $\zeta_1^{(1)}$, and (A.5a) for $Q_1^{(2)}$.

---

* Although the operator on the homogeneous part of (A.5) is singular, a solution exists nevertheless, because the homogeneous and inhomogeneous parts are orthogonal owing to the value taken by σ_1 in (5.15).

The end-point value of ζ_1 for integration of (A.5b) is chosen to make end values of Q_1 vanish upon integration of (A.5a).

For numerical computation the derivatives in (A.5) are replaced by finite differences, in the manner explained in section 2. It should be remarked also that in the foregoing analysis, the differential rather than the difference equations have been used for the sake of brevity; however, exactly the same analysis can be carried out from the difference equations. Modifications required for Long Point Bay are rather apparent and need not be stressed.

B. Derivation of (5.23)

Expand S and σ, ζ, Q in powers of the real quantity δh. Then $S_1 = b$, and we find that the zero-order and first-order statements of (A.1) are $K_0 - P_0 = 0$ as in (A.2a), and $K_1 - P_1 = 0$ in place of (A.2b). However, the latter may be written

$$K_1' - P_1 = W_0 \qquad (B.1)$$

$$K_1' \equiv \int_0^L \frac{Q_0 Q_1}{S}\, dx$$

From equations (1a) and (0b) of Appendix A we get

$$\sigma_1 P_0 + \tfrac{1}{2}\sigma_0 (P_1 - K_1') = 0$$

in place of (A.4); hence from (B.1) we get (5.23) directly.

C. Derivation of (5.26)

Starting from (5.11) --- without the friction term, but with end conditions (5.25), the result of performing the operations that gave (A.1) is

$$\sigma(K-P) = -i\lambda Z \qquad (C.1)$$

$$Z \equiv \tfrac{1}{2} g(\zeta^2)_{x=0} \ ,$$

which formally is identical to (A.1), with ku replaced by λ and W by $-Z$. Expansion in powers of $i\lambda$ then leads to (A.2) with W replaced by $-Z$, and to (0a, b), (1a, b), (2a, b) with the friction terms absent.

Continuing with this process, we find that the operations leading to (A.4) now give

$$\sigma_1 P_0 + \tfrac{1}{2}\sigma_0 (P_1 - K_1) = Z_0 \ .$$

From (A.2a, b) (with W_0 replaced by $-Z_0$) we find (5.26).

REFERENCES

Corkan, R. H. and A. T. Doodson, 1952: Free tidal oscillations in a rotating square sea. Proceedings, Royal Society of London, Series A, 147-162.

Darwin, Sir George H., 1911: The tides and kindred phenomena in the solar system. London, John Murray, 437 pp.

Defant, A., 1961: Physical oceanography. London, Pergamon Press, volume 2, 598 pp.

Defant, F., 1954: Theorie der Seiches des Michigansees und ihre Abwendlung durch Wirkung der Corioliskraft. Archiv für Meteorologie, Geophysik und Bioklimatologie, 6, 218-241.

Endrös, A., 1908: Vergleichende Zusammenn-stellung der Hauptseiches-perioden der bis jetzt untersuchten Seen mit Anwendung auf verwandte Probleme. Petermanns Mitteilungen, 54, 60-68.

Goldsbrough, G. R., 1931: The tidal oscillations in an elliptic basin of variable depth. Proceedings, Royal Society of London, Series A, 130, 157-167.

Goldstein, S., 1928: The free oscillations of water in a canal of elliptic plan. Proceedings, London Mathematical Society, Series 2, 28, 91-101.

Goldstein, S., 1929: Tidal motion in rotating elliptic basins of constant depth. Monthly Notices, Royal Astronomical Society, Geophysical Supplement, 2, 213-231.

Green, Charles K., 1960: "Physical hydrography and temperature," in Limnological survey of Eastern and Central Lake Erie, 1928-1929, by Charles J. Fish and Associates. U. S. Fish and Wildlife Service, Special Scientific Report, Fisheries number 334, 11-73.

Hayford, John F., 1922: Effects of winds and barometric pressures on the Great Lakes. Carnegie Institution of Washington, 133 pp.

Henry, Alfred J., 1902: Wind velocity and fluctuations of water level on Lake Erie. U. S. Weather Bureau, Bulletin J, 22 pp.

Hidaka, Koji, 1931: The oscillations of water in spindle-shaped and elliptic basins as well as the associated problems (Problems of water oscillations in various types of basins and canals - Part I). Memoirs, Imperial Marine Observatory of Kobe, 4 (2), 99-220.

Hunt, Ira A., Jr., 1959: Winds, wind set-ups and seiches on Lake Erie. U. S. Lake Survey, Corps of Engineers, 58 pp.

Hutchinson, G. Evelyn, 1957: A treatise on limnology. New York, John Wiley and Sons, volume 1, 1015 pp.

Jeffreys, H., 1925: The free oscillations of water in an elliptical lake. Proceedings, London Mathematical Society, Series 2, 23, 455-476.

Keulegan, Garbis H., 1959: Energy dissipation in standing waves in rectangular basins. Journal of Fluid Mechanics, 6, 33-50.

Lamb, Sir Horace, 1924: Hydrodynamics, 5th edition. Cambridge University Press, 687 pp.

_____, 1932: Hydrodynamics, 6th edition. Cambridge University Press, 738 pp.

Mortimer, C. H., 1955: Some effects of the earth's rotation on water movement in stratified lakes. Verhandlungen der internationalen Vereinigung für theoretische und angewandte Limnologie, 12, 66-77.

Neumann, Gerhard, 1942: Periodische Strömungen im Finnischen Meerbusen im Zusammenhang mit den Eigenschwingungen der Ostsee. Gerlands Beiträge zur Geophysik, 59, 1-15.

Olson, F. C. W., 1950: The currents of western Lake Erie. Ohio State University, Ph.D. thesis, 370 pp.

Platzman, George W. and Desiraju B. Rao, 1963: Spectra of Lake Erie water levels (to be published).

Platzman, George W., 1963: The dynamical prediction of wind tides on Lake Erie. Meteorological Monographs (in press).

Proudman, J. and A. T. Doodson, 1924: Time relations in meteorological effects on the sea. Proceedings, London Mathematical Society, 24, 140-149.

Lord Rayleigh, 1903: On the vibrations of a rectangular sheet of rotating liquid. Philosophical Magazine, 5, 297-301.

_____, 1909: Notes concerning tidal oscillations upon a rotating globe. Proceedings, Royal Society of London, Series A, 82, 448-464.

Taylor, G. I., 1922: Tidal oscillations in gulfs and rectangular basins. Proceedings, London Mathematical Society, Series 2, 20, 148-181.

Van Dantzig, D. and H. A. Lauwerier, 1962: The North Sea problem IV. Free oscillations of a rotating rectangular sea. Proceedings, Koninklijke Nederlandske Akadamie Van Wetenschappen, Series A, 63, 339-354.

Verber, James L., 1960: Long and short period oscillations in Lake Erie. State of Ohio, Department of Natural Resources, Division of Shore Erosion, 80 pp.

Whipple, George C., 1927: The microscopy of drinking water. New York, John Wiley & Sons, 586 pp.

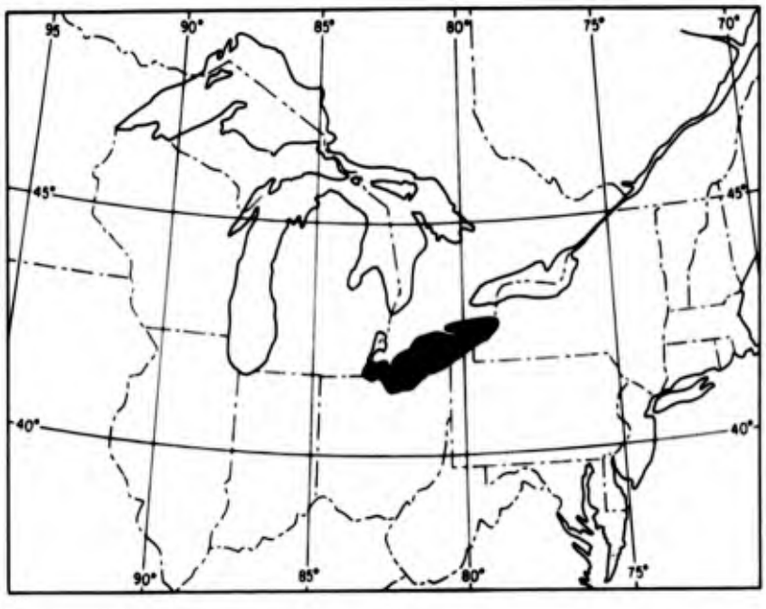

Figure 1. Lake Erie location map.

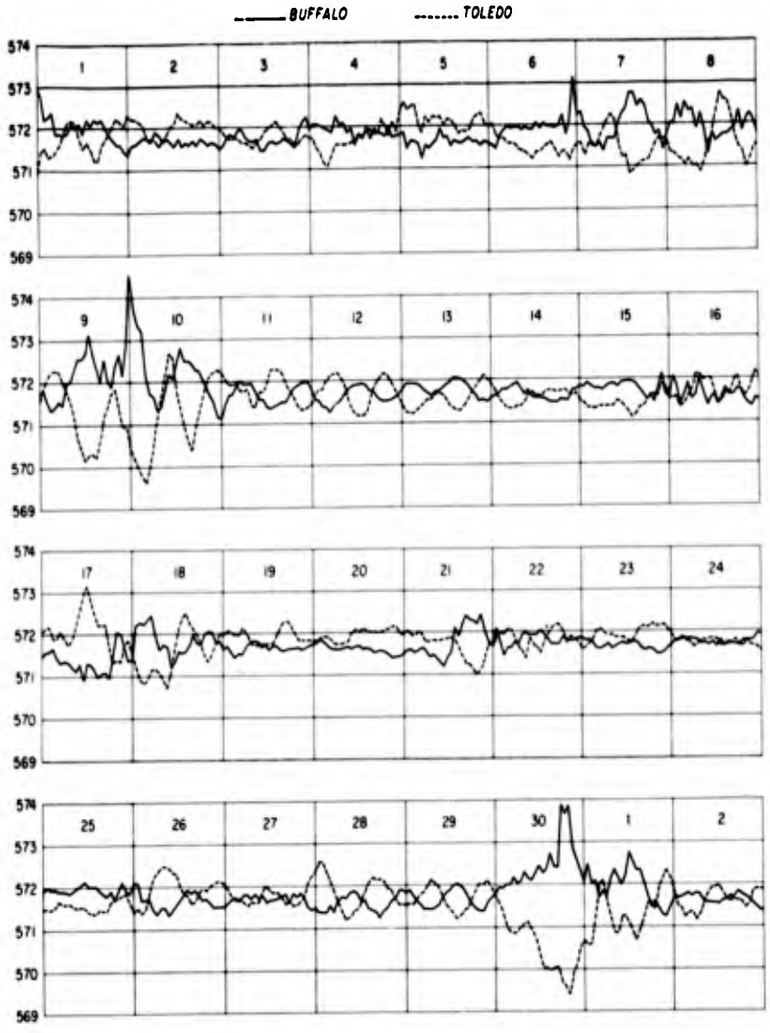

Figure 2. Hourly scaled lake levels (in feet MSL) at Buffalo (solid line) and Toledo (broken line) from 1 September through 2 October 1958.

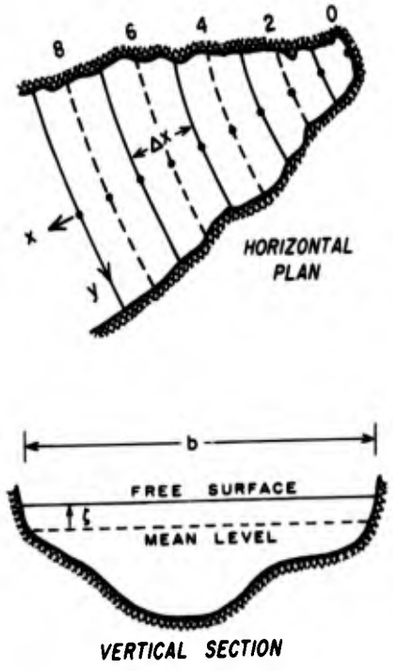

Figure 3. Schematic picture of horizontal plan and vertical section in gradually varying channel. Dotted line in horizontal plan is principal axis; solid lines are profile (ζ) sections, broken lines are transport (Q) sections.

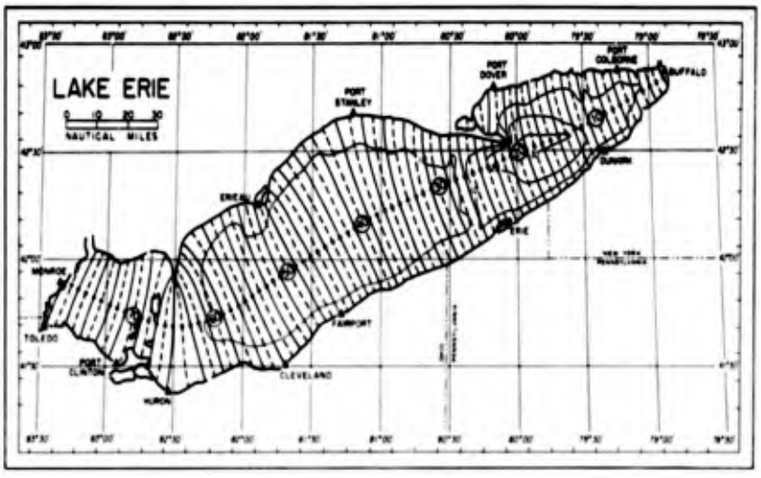

Figure 4. Bathymetric contours at 10-fathom intervals (1 fathom = 6 feet); principal axis (dotted line); normal sections: solid lines are profile (ζ) sections, broken lines are transport (Q) sections; locations (▲) of lake-level recorders.

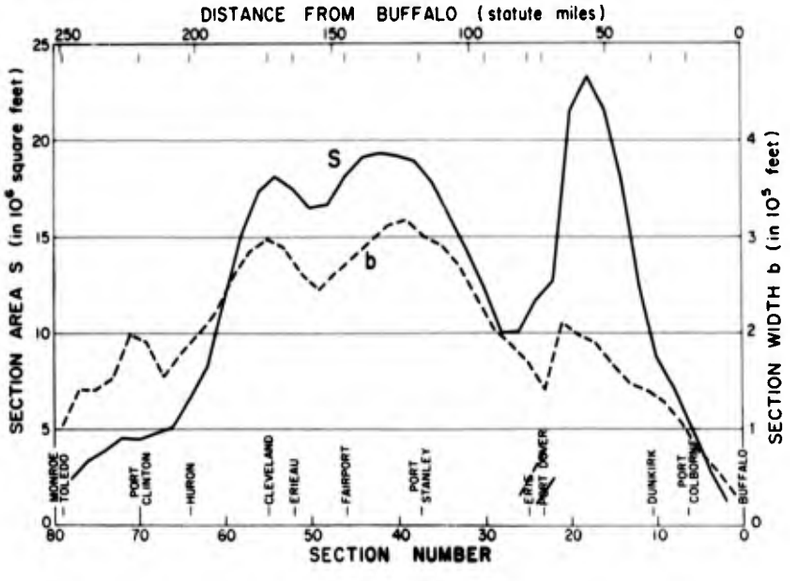

Figure 5. Area (S) and surface width (ℓ) of sections defined in figure 4. Upper scale gives distance from Buffalo along principal axis; locations of lake-level recorders are shown above lower scale.

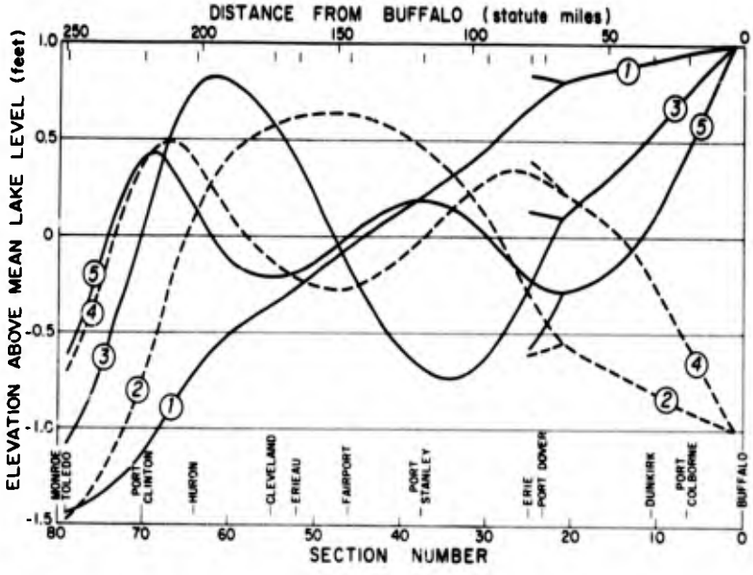

Figure 6. Computed lake-level profiles for the first five modes of longitudinal free oscillation of Lake Erie. Each mode is assigned an amplitude of 1.0 ft at Buffalo. The short segments between sections 21 and 25 represent profiles in Long Point Bay.

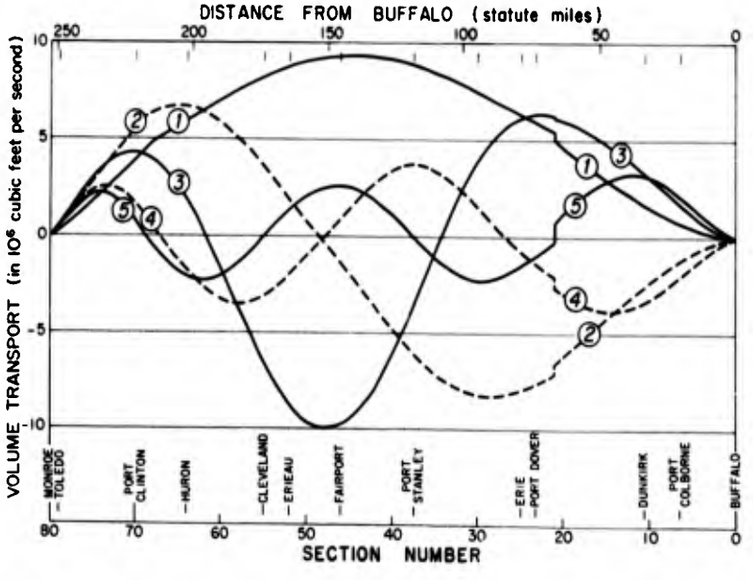

Figure 7. Computed volume transport. The jumps at section 21 correspond to transport through the mouth of Long Point Bay.

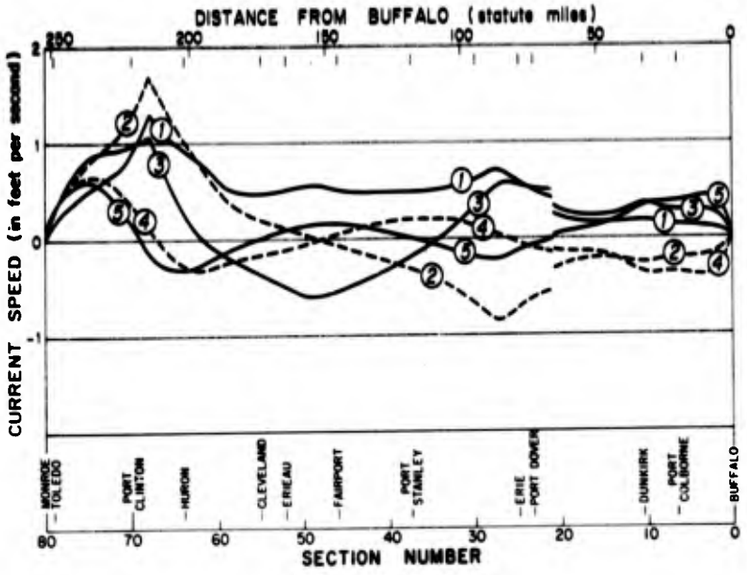

Figure 8. Computed current speed.

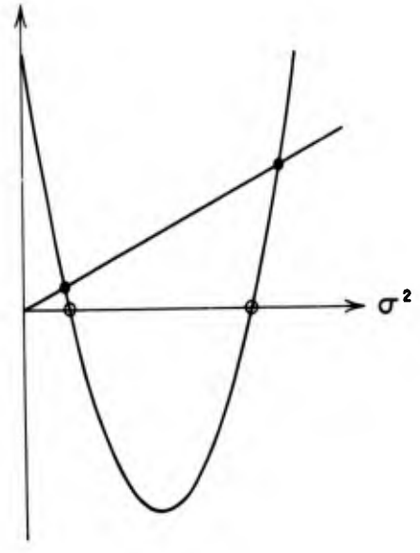

Figure 9. Graphical representation of roots of (5.6): parabola is left side of equation, straight line is right side. Open circles are σ_L^2 ; σ_β^2 ; black dots show roots of (5.6).

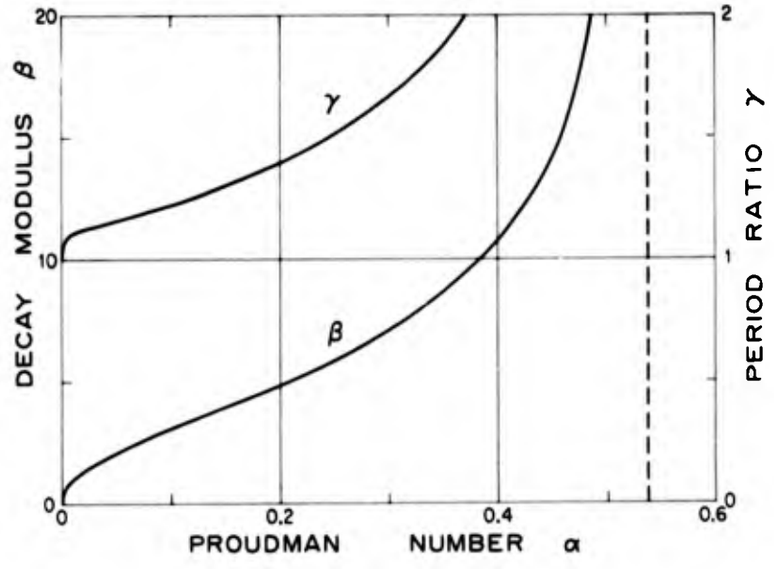

Figure 10. Period ratio (γ) and decay modulus (β) as a function of Proudman number (α).

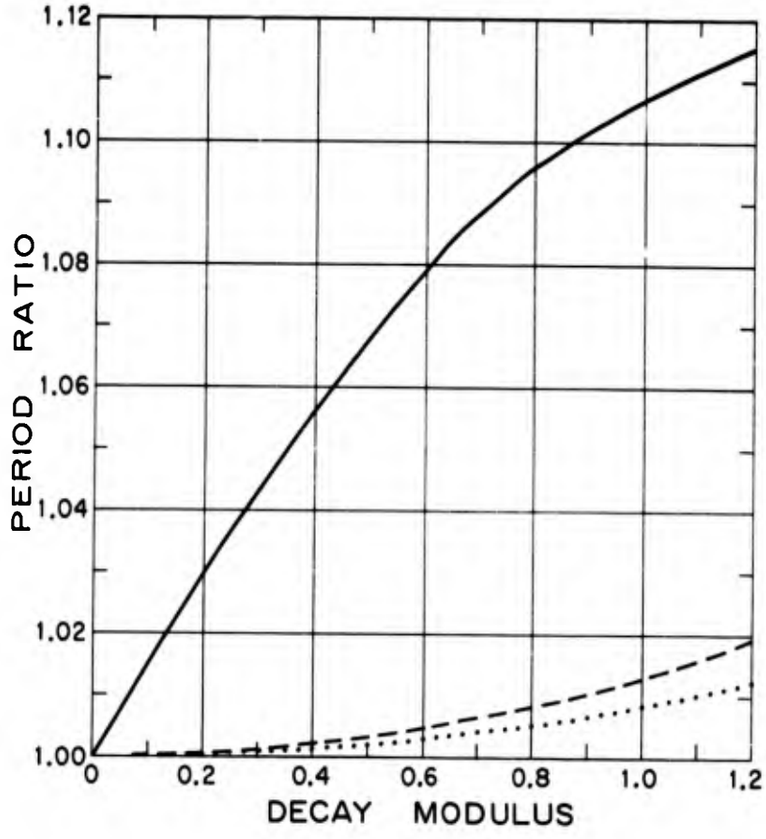

Figure 11. Period ratio as a function of decay modulus. Solid curve: from Proudman and Doodson's (1924) theory; broken curve: for linear skin friction in a rectangular basin of uniform depth; dotted curve: for linear skin friction in Lake Erie.

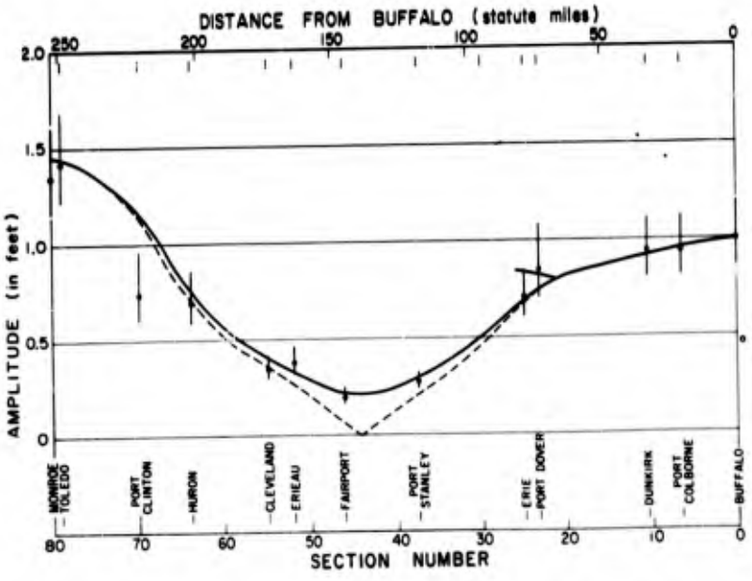

Figure 12. Computed amplitude of the first mode with rotation (solid curve) and without rotation (broken curve). Dots show observed amplitude estimated from spectral analyses. Vertical bars show 95 per cent confidence limits.

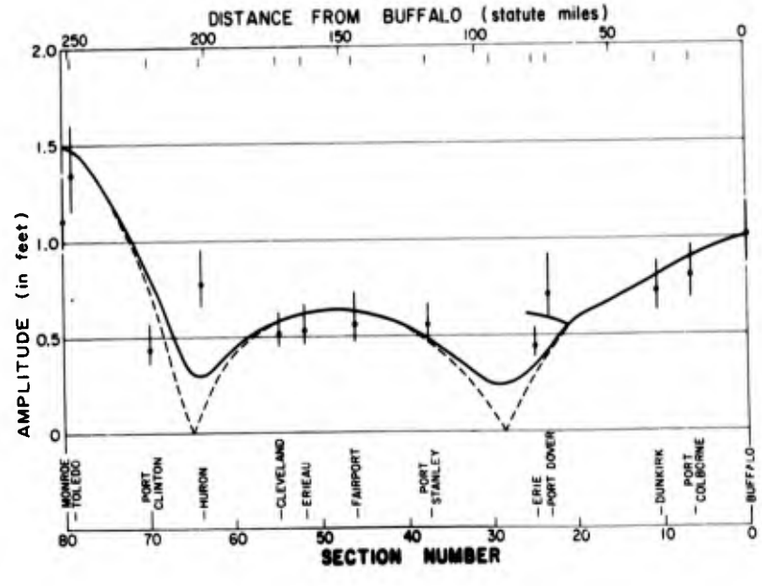

Figure 13. Computed and observed amplitudes of second mode.

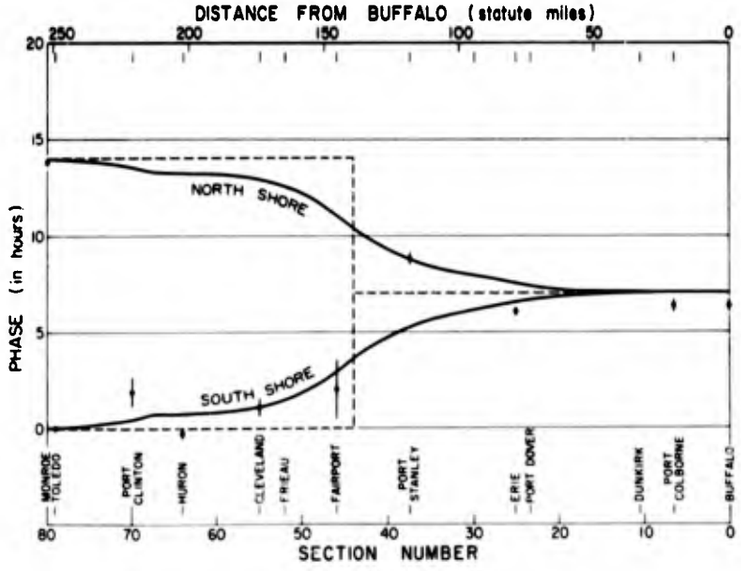

Figure 14. Computed phase of the first mode with rotation (solid curve) and without rotation (broken curve). Dots show observed phase estimated from cross-spectral analyses. Vertical bars show 95 per cent confidence limits..

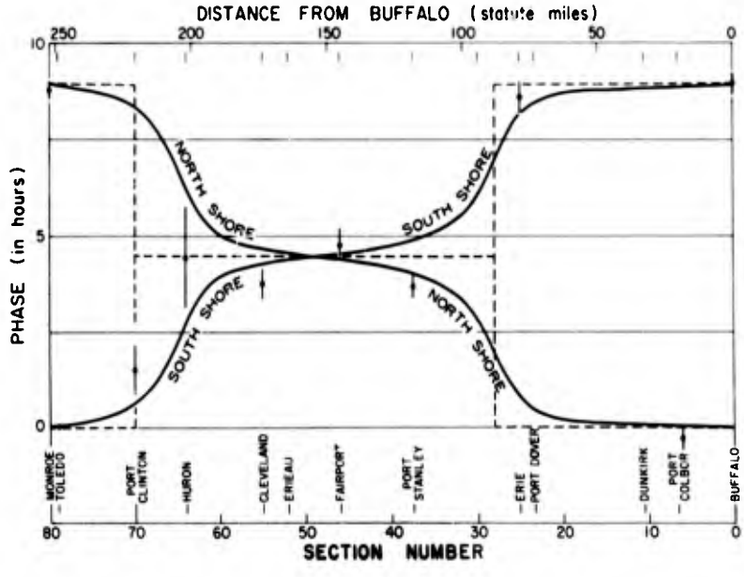

Figure 15. Computed and observed phases of second mode.

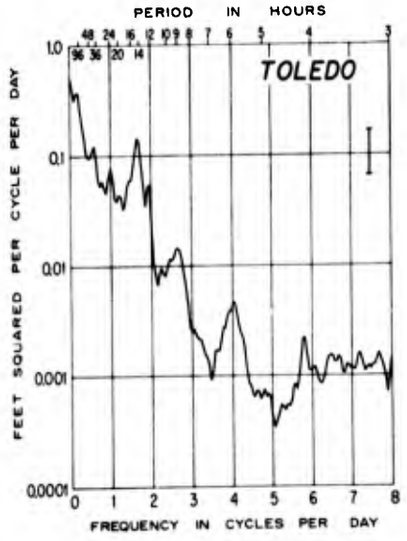

Figure 16. Covariance spectrum of hourly lake levels at Toledo, 1 April through 30 September 1958; frequency resolution, 0.05 cycle per day (from Platzman and Rao, 1963).

(continued from inside front cover)

*16a. Lester F. Hubert: A test of numerical hurricane prediction under operational conditions. (Technical Report to U. S. Weather Bureau, January 1959). Equivalent to number 16b (see below).

16b. Lester F. Hubert: An operational test of a numerical prediction method for hurricanes. Monthly Weather Review, 87 (1959) 222-230.

17. George W. Platzman: The spectral form of the vorticity equation. (Technical Report to National Science Foundation, June 1959). Journal of Meteorology 17 (1960) 635-644.

18. Akira Kasahara: The numerical prediction of hurricane movement with a two-level baroclinic model. (Technical Report to U. S. Weather Bureau, August 1959). Journal of Meteorology, 17 (1960) 357-370.

*19a. John M. Mihaljan: A rigorous derivation of the Boussinesq approximations in the hydrodynamical equations. (Technical Report to National Science Foundation, February 1960). Equivalent to number 19b (see below).

+19b. John M. Mihaljan: A rigorous exposition of the Boussinesq approximations in the hydrodynamical equations. Ph.D. Thesis, September 1960.

19c. John M. Mihaljan: A rigorous exposition of the Boussinesq approximations applicable to a thin layer of fluid. The Astrophysical Journal, 136 (1962) 1126-1133.

*20a. Hsiao-lan Kuo and George W. Platzman: An investigation of the nonlinear solution of the Rayleigh convection problem by means of characteristic functions. (Technical Report to National Science Foundation, March 1960). Equivalent to number 20b (see below).

20b. Hsiao-lan Kuo and George W. Platzman: A normal mode nonlinear solution of the Rayleigh convection problem. Beiträge zur Physik der Atmosphäre, 33 (1961) 137-168.

+21. Robert W. Jones: The tracking of hurricane Audrey 1957 by numerical prediction. (Technical Report to U. S. Weather Bureau, March 1960). M.S. Thesis, March 1960. Journal of Meteorology, 18 (1961) 127-138.

22. Akira Kasahara: A numerical experiment on the development of a tropical cyclone. (Technical Report to U. S. Weather Bureau, April 1960). Journal of Meteorology, 18 (1961) 259-282.

23. Gene E. Birchfield: Numerical prediction of hurricane movement with the equivalent-barotropic model. (Technical Report to U. S. Weather Bureau, July 1960). Journal of Meteorology, 18 (1961) 402-409.

24. Ferdinand Baer and George W. Platzman: A procedure for numerical integration of the spectral vorticity equation. (Technical Report to National Science Foundation, July 1960). Journal of Meteorology, 18 (1961) 393-401.

25. Akira Kasahara: The development of forced convection caused by the released latent heat of condensation in a hydrostatic atmosphere. (Technical Report to U. S. Weather Bureau, December 1960). Proceedings of the International Symposium on Numerical Weather Prediction in Tokyo, 387-401. Meteorological Society of Japan, 1962.

26. Shirley M. Irish and George W. Platzman: An investigation of the meteorological conditions associated with extreme wind tides on Lake Erie. (Technical Report to U. S. Weather Bureau, May 1961). Monthly Weather Review, 90 (1962) 39-47.

*27. Robert W. Jones: An objective technique for removing a cyclonic vortex pattern from a two-dimensional field of data at equally spaced grid points. (Technical Report to U. S. Weather Bureau, July 1961).

*28. Akira Kasahara: A study of stability of thermally driven and frictionally controlled symmetrical motions with application to the mechanism for development of tropical cyclones. (Technical Report to U. S. Weather Bureau, August 1961).

(continued on outside back cover)

(continued from inside back cover)

*29a. Ferdinand Baer: Incegration with the spectral vorticity equation. (Technical Report to National Science Foundation, September 1961). Equivalent to number 29b (see below).

+29b. Ferdinand Baer: Some properties of the spectral vorticity equation. Ph.D. Thesis, December 1961.

*30. Shirley M. Irish: The surge of 3 August 1960 on Lake Michigan. (Technical Report to U. S. Weather Bureau, October 1961).

31. George W. Platzman: The analytical dynamics of the spectral vorticity equation. (Technical Report to National Science Foundation, January 1962). Journal of Atmospheric Sciences, 19 (1962) 313-328.

+32a. Gene E. Birchfield: Some dynamical properties of free oscillations of the atmosphere of the second class. Ph.D. Thesis, June 1962.

*32b. Gene E. Birchfield: Some properties of free atmospheric oscillations of the second class. (Technical Report to National Science Foundation, August 1962). Equivalent to number 32a (see above).

+33. Desiraju B. Rao: The response of a lake to a time-dependent wind stress. (Technical Report to U. S. Weather Bureau, June 1962). M.S. Thesis, August 1962.

34. Frank B. Lipps: Stability of jets in a divergent barotropic fluid. (Technical Report to National Science Foundation, July 1962). Journal of the Atmospheric Sciences, 20 (1963) 120-129.

35. George W. Platzman: The dynamical prediction of wind tides on Lake Erie. (Technical Report to U. S. Weather Bureau, December 1962).

36. Robert W. Jones: On improving initial data for numerical forecasts of hurricane trajectories by the steering method. (Technical Report to U. S. Weather Bureau, March 1963).

37. Akira Kasahara and George W. Platzman: Interaction of a hurricane with the steering flow and its effect upon the hurricane trajectory. (Technical Report to U. S. Weather Bureau, April 1963).

+38. John M. Lewis: The present state of knowledge of the Great Lakes currents. M.S. Thesis, June 1963.

UNCLASSIFIED